Periodic Updates for Constrained OCO with Application to Large-Scale Multi-Antenna Systems

Juncheng Wang, *Student Member, IEEE*, Min Dong, *Senior Member, IEEE*, Ben Liang, *Fellow, IEEE*, and Gary Boudreau, *Senior Member, IEEE*

arXiv:2103.02124v2 [cs.IT] 12 Jul 2021

Abstract

In many dynamic systems, decisions on system operation are updated over time, and the decision maker requires an online learning approach to optimize its strategy in response to the changing environment. When the loss and constraint functions are convex, this belongs to the general family of online convex optimization (OCO). In existing OCO works, the environment is assumed to vary in a time-slotted fashion, while the decisions are updated at each time slot. However, many wireless communication systems permit only periodic decision updates, *i.e.,* each decision is fixed over multiple time slots, while the environment changes between the decision epochs. The standard OCO model is inadequate for these systems. Therefore, in this work, we consider periodic decision updates for OCO. We aim to minimize the accumulation of time-varying convex loss functions, subject to both short-term and long-term constraints. Information about the loss functions within the current update period may be incomplete and is revealed to the decision maker only after the decision is made. We propose an efficient algorithm, termed Periodic Queueing and Gradient Aggregation (PQGA), which employs novel periodic queues together with possibly multi-step aggregated gradient descent to update the decisions over time. We derive upper bounds on the dynamic regret, static regret, and constraint violation of PQGA. As an example application, we study the performance of PQGA in a large-scale multi-antenna system shared by multiple wireless service providers. Simulation results show that PQGA converges fast and substantially outperforms the known best alternative.

Index Terms

Online convex optimization, long-term constraint, periodic updates, massive MIMO, wireless network virtualization.

J. Wang and B. Liang are with the University of Toronto (e-mail: {jcwang, liang}@ece.utoronto.ca). M. Dong is with the Ontario Tech University (e-mail: min.dong@ontariotechu.ca). G. Boudreau is with Ericsson Canada (e-mail: gary.boudreau@ericsson.com). This work has been funded in part by Ericsson Canada and by the Natural Sciences and Engineering Research Council (NSERC) of Canada. A preliminary version of this work has appeared in IEEE SPAWC [1].

I. Introduction

In many signal processing, resource allocation, and machine learning problems, system parameters and loss functions vary over time under dynamic environments. Online learning has emerged as a promising solution to these problems in the presence of uncertainty, where an online decision strategy iteratively adapts to system variations based on historical information [2]. Online convex optimization (OCO) is a subclass of online learning, where the loss and constraint functions are convex with respect to (w.r.t.) the decision [3]. OCO can be seen as a sequential decision-making process between a decision maker and the system. Under the standard OCO setting, at the beginning of each time slot, the decision maker selects a decision from a convex feasible set. Only at the end of each time slot, the system reveals information about the current convex loss function to the decision maker. The goal of the decision maker is to minimize the cumulative loss. Such an OCO framework has many applications, *e.g.,* wireless transmit covariance matrix design [4], dynamic network resource allocation [5], and smart grids with renewable energy supply [6].

In OCO, due to the lack of in-time information about the current convex loss function, the decision maker cannot select an optimal decision at each time slot. Instead, the decision maker aims at minimizing the *regret* [7], *i.e.,* the performance gap between the online decision sequence and some performance benchmark. Most of the early OCO algorithms were evaluated in terms of the *static* regret, which compares the online decision sequence with a static offline benchmark that has apriori information of all the convex loss functions. However, when the environment changes drastically, the static offline benchmark itself may perform poorly. In this case, the static regret may not be a meaningful performance measurement anymore. A more useful *dynamic* regret measures the performance gap between the online decision sequence and a time-varying sequence of per-time-slot optimizers given knowledge of the current convex loss function. The dynamic regret has been recognized as a more attractive but harder-to-track performance measurement for OCO.

In many practical systems, the decision maker often collects the system parameters and makes decisions in a *periodic* manner, *e.g.,* to limit the computation and communication overhead. One application of interest is precoding design in massive multiple-input multiple-output (MIMO) systems, where the precoder is updated based on delayed channel state information (CSI) feedback and is fixed for a period, *i.e.,* one or multiple resource block durations, while the

underlying channel can fluctuate quickly over time. The resource block duration is fixed in Long-Term Evolution (LTE) and is allowed to change over time for a more flexible network operation in 5G New Radio (NR) [8]. In mobile edge computing [9], due to the offloading and scheduling latency, the cloud server may periodically collect the offloading tasks from the remote devices and design a fixed computing resource allocation strategy for a certain time period.

However, to the best of our knowledge, all existing works on OCO require both the decision and feedback information are updated at each time slot. Motivated by this discrepancy, in this work, we consider a new constrained OCO problem with *periodic updates*, where the decision maker periodically collects information feedbacks and makes online decisions to minimize the accumulated loss. The duration of update period can be multiple time slots and can vary over time. In the presence of periodic updates, no existing work provides regret bound analysis for OCO.

Furthermore, we consider both short-term and long-term constraints, which are important in many practical optimization problems. For example, in communication systems, the short-term constraint can represent the maximum transmit power, while the long-term power constraint can be seen as a limit on energy usage. An effective constrained OCO algorithm should also bound the *constraint violation*, which is the accumulated violation on the long-term constraints. The need to provide the constraint violation bound further adds to the challenges of regret bound analysis.

The main contributions of this paper are as follows:

- We formulate a new constrained OCO problem with periodic updates. Each update period may last for multiple time slots and may vary over time. At the beginning of each update period, the decision maker selects a decision, fixed for the period, to minimize the accumulated loss subject to both short-term and long-term constraints. The feedback information about the loss functions can be delayed for multiple time slots and partly missing. As explained above, this constrained OCO framework with periodic updates has broad applications in practical communication and computation systems.
- We propose an efficient algorithm, termed Periodic Queueing and Gradient Aggregation (PQGA) for the formulated constrained OCO problem. In PQGA, we propose a novel construction of *periodic queues*, which converts the accumulated constraint violation in an update period into queue dynamics. Furthermore, PQGA collects and aggregates the delayed gradient feedbacks in each update period. The periodic queues, together with gradient

aggregation, improve the efficacy of periodic decision updates and facilitate the performance bounding of PQGA.

- We analyze the performance of PQGA and study the impact of the periodic queues and gradient aggregation. We prove that PQGA yields $\mathcal{O}(\max\{T^{\frac{1+\nu}{2}}, T^{\delta+\kappa}\})$ dynamic regret, $\mathcal{O}(\max\{T^{\frac{1}{2}}, T^{\delta+\kappa}\})$ static regret, and $\mathcal{O}(T^{\frac{1}{2}-\kappa})$ constraint violation, where T is the total time horizon, ν represents the growth rate of the accumulated variation of the per-time-slot optimizer, δ measures the level of variation of the update period, and $\kappa \in [0, \frac{1}{2}]$ is a tunable trade-off parameter. We further show that, when the number of gradient descent steps within each update period is large enough, PQGA provides improved $\mathcal{O}(\max\{T^{\nu}, T^{\delta}\})$ dynamic regret and $\mathcal{O}(1)$ constraint violation. For the special case of per-time-slot updates, PQGA achieves $\mathcal{O}(T^{\nu})$ dynamic regret and $\mathcal{O}(1)$ constraint violation bound.
- As an application, we use PQGA to solve an online precoding design problem in massive MIMO systems with multiple wireless service providers, where all the antennas and wireless spectrum resources are simultaneously shared by the service providers. In this case, we show that PQGA only involves low-complexity closed-form computation. Simulation results show that PQGA converges fast and substantially outperforms the known best alternative.

Organizations: The rest of this paper is organized as follows. In Section II, we present the related work. Section III describes the mathematical model, problem formulation, and performance measurement for constrained OCO with periodic updates. We present PQGA, derive its performance bounds, and discuss its performance merits in Section IV. The application of PQGA to large-scale multi-antenna systems with multiple wireless service providers is presented in Section V. Simulation results are provided in Section VI, followed by concluding remarks in Section VII.

Notations: The transpose, Hermitian transpose, complex conjugate, trace, Euclidean norm, Frobenius norm, L_∞ norm, and L_1 norm of a matrix $\mathbf{A}$ are denoted by $\mathbf{A}^T$, $\mathbf{A}^H$, $\mathbf{A}^*$, $\mathrm{tr}\{\mathbf{A}\}$, $\|\mathbf{A}\|$, $\|\mathbf{A}\|_F$, $\|\mathbf{A}\|_\infty$, and $\|\mathbf{A}\|_1$, respectively. The notation $\mathrm{blkdiag}\{\mathbf{A}_1, \ldots, \mathbf{A}_n\}$ denotes a block diagonal matrix with diagonal elements being matrices $\mathbf{A}_1, \ldots, \mathbf{A}_n$, $\mathbb{E}\{\cdot\}$ denotes expectation, $\Re\{\cdot\}$ denotes the real part of the enclosed parameter, $\mathbf{I}$ denotes an identity matrix, and $\mathbf{g} \sim \mathcal{CN}(\mathbf{0}, \sigma^2\mathbf{I})$ means that $\mathbf{g}$ is a circular complex Gaussian random vector with mean $\mathbf{0}$ and variance $\sigma^2\mathbf{I}$.

TABLE I
SUMMARY OF RELATED WORKS ON OCO

Reference	Type of benchmark	Long-term constraint	Periodic updates
[7]	Static and dynamic	No	No
[10]-[12]	Static	No	No
[13]-[17]	Dynamic	No	No
[18]-[20], [22], [23]	Static	Yes	No
[21], [24]	Dynamic	Yes	No
[25]	Static and dynamic	Yes	No
PQGA	Static and dynamic	Yes	Yes

II. RELATED WORK

In this section, we survey existing works on OCO. The differences between the existing literature and our work are summarized in Table I.

A. Online Learning and OCO

Online learning is a method of machine learning, where a learner attempts to tackle some decision-making task by learning from a sequence of data instances. As an important subclass of online learning, OCO has been applied in various areas such as wireless communications [4], cloud networks [5], and smart grids [6]. In the seminal work of OCO [7], a simple projected gradient descent algorithm achieved $\mathcal{O}(T^{\frac{1}{2}})$ static regret [7]. The static regret was further improved to $\mathcal{O}(\log T)$ for strongly convex loss functions [10]. Moreover, [11] and [12] examined the static regret for OCO where information feedbacks of the loss functions are delayed for multiple time slots.

The analysis of static regret was extended to that of the more attractive dynamic regret in [7], [13], [14] for general convex loss functions. Moreover, strongly convexity was shown to improve the dynamic regret bound in [15]. By increasing the number of gradient descent steps, the dynamic regret bound was further improved in [16]. Furthermore, [17] studied the impact of inexact gradient on the dynamic regret bound.

B. OCO with Long-Term Constraints

The above OCO works [7], [10]-[17] focused on online problems with short-term constraints represented by a feasible set that must be strictly satisfied. However, long-term constraints arise in many practical applications such as energy control in wireless communications, queueing

stability in cloud networks, and power balancing in smart grids. Existing algorithms for OCO with long-term constraints can be categorized into saddle-point-typed algorithms [18]-[21] and virtual-queue-based algorithms [22]-[25].

A saddle-point-typed algorithm was first proposed in [18] and achieved $\mathcal{O}(T^{\frac{1}{2}})$ static regret and $\mathcal{O}(T^{\frac{3}{4}})$ constraint violation. A follow-up work [19] provided $\mathcal{O}(T^{\max\{\mu,1-\mu\}})$ static regret and $\mathcal{O}(T^{1-\frac{\mu}{2}})$ constraint violation, where $\mu \in (0,1)$ is some trade-off parameter. This recovers the performance bounds in [18] as a special case. In the presence of multi-slot delay, [20] achieved $\mathcal{O}(T^{\frac{1}{2}})$ static regret and $\mathcal{O}(T^{\frac{3}{4}})$ constraint violation. The saddle-point-typed algorithm was further modified in [21] with dynamic regret analysis.

As an alternative to saddle-point-typed algorithms, virtual queues can be used to represent the backlog of constraint violation, which facilitates performance bounding through the analysis of a drift-plus-penalty (DPP) like expression. A virtual-queue-based algorithm was first proposed in [22] and established $\mathcal{O}(T^{\frac{1}{2}})$ static regret and $\mathcal{O}(1)$ constraint violation for OCO with fixed long-term constraints. For stochastic constraints that are independent and identically distributed (i.i.d.), another virtual-queue-based algorithm in [23] achieved $\mathcal{O}(T^{\frac{1}{2}})$ static regret and $\mathcal{O}(T^{\frac{1}{2}})$ constraint violation simultaneously. In [24], the virtual-queue-based algorithm was further extended to provide a dynamic regret bound. The impact of multi-slot feedback delay on constrained OCO was considered in [25] with both dynamic and static regret analyses.

However, all of the above works on constrained OCO [18]-[25] are under the standard per-time-slot update setting. No other known work considers periodic updates for OCO. Furthermore, these works only performs single-step gradient descent at each time slot, which does not take full advantage of the potential computational capacity to improve the system performance. In this paper, we propose PQGA, which uses novel periodic queues with possibly multi-step aggregated gradient descent to update the online decision. We believe this is the first of its kind.

A part of this work has appeared as a short paper that focuses only on the application of constrained OCO with period updates to large-scale multi-antenna systems [1]. In the current manuscript, we have substantially extended our prior work, generalizing the PQGA algorithm, accommodating multi-step gradient descent, deriving new regret and constraint violation bounds over time-varying update periods, and providing other new derivations, proofs, and simulation results.

C. Lyapunov Optimization

PQGA is substantially different from the conventional DPP algorithm for Lyapunov optimization [26] in both the decision update and the virtual queue update. Lyapunov optimization makes use of the system state and queueing information to implicitly learn and adapt to system variation with unknown statistics. The standard Lyapunov optimization is confined to per-time-slot updates [26]. It was extended in [27] to accommodate variable renewal frames. However, under this framework, the system states are commonly assumed to be i.i.d. or Markovian, while the OCO framework does not have such restriction. Furthermore, [27] assumes the system state to be fixed within each renewal frame, while we allow the loss function to change at each time slot within an update period.

In addition, the standard Lyapunov optimization relies on the current and accurate system state for decision updates [26]. When the system state feedback is delayed, one can apply Lyapunov optimization by leveraging the historical information to predict the current system state with some error [28]. However, this way of dealing with feedback delay is equivalent to extending Lyapunov optimization to inaccurate system states [29], [30]. In this case, the optimality gap would be $\mathcal{O}(\sigma T)$, where σ is some inaccuracy measure.

III. Constrained OCO with Periodic Updates

In this section, we detail the mathematical model of constrained OCO with periodic updates, and we present the formulation of the static regret, dynamic regret, and constraint violation for performance measurement.

A. OCO Problem Formulation

We consider a time-slotted system with time indexed by t. Let $f_t(\mathbf{x}) : \mathbb{R}^n \to \mathbb{R}$ be a loss function at time slot $t \in \mathcal{T} = \{0, \ldots, T-1\}$. The loss function $f_t(\mathbf{x})$ is convex and can change arbitrarily over time. Let $\mathbf{x}_t \in \mathbb{R}^n$ be the decision vector at time slot t. Let $\mathcal{X}_0 \subseteq \mathbb{R}^n$ be a compact convex set that represents the short-term constraints for any $\mathbf{x}_t$, $t \in \mathcal{T}$. The goal of the decision maker is to minimize the accumulated loss $\sum_{t\in\mathcal{T}} f_t(\mathbf{x}_t)$.

In standard OCO, the decision maker can update $\mathbf{x}_t$ for any $t \in \mathcal{T}$. As explained above, this often is not possible in many practical systems. Therefore, in this paper, we consider periodic decision updates for OCO. Suppose the time horizon of T time slots is segmented into I update periods, as shown in Fig. 1. Each update period $i \in \mathcal{I} = \{0, \ldots, I-1\}$ has a duration of

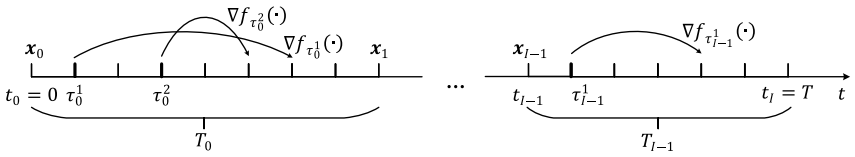


Fig. 1. A timeline illustrating OCO with periodic updates.

$T_i \in \{1, \ldots, T_{\max}\}$ time slots with $T_{\max}$ being the maximum duration of an update period. We have $T = \sum_{i \in \mathcal{I}} T_i$. Let t_i represent the beginning time slot of update period i. The decision vector is updated at the beginning of time slot t_i. For convenience of exposition, we slightly abuse the notation and use $\mathbf{x}_i$ to denote this decision vector. It remains unchanged within update period i, *i.e.,* $\mathbf{x}_t = \mathbf{x}_i$ for any $t \in \mathcal{T}_i = \{t_i, t_i + 1, \ldots, t_i + T_i - 1\}$, $i \in \mathcal{I}$. Under this new per-period update setting, the accumulated loss becomes $\sum_{i \in \mathcal{I}} \sum_{t \in \mathcal{T}_i} f_t(\mathbf{x}_i)$.

Let $\nabla f_t(\cdot)$, $t \in \mathcal{T}_i$, be the possible gradient information within update period i. Assume that there are $S_i \in \{1, \ldots, T_i\}$ gradient feedbacks received by the decision maker within update period i. Let τ_i^s, for $s \in \mathcal{S}_i = \{1, \ldots, S_i\}$, represent the time slot at which the s-th gradient feedback in update period i, denoted by $\nabla f_{\tau_i^s}(\cdot)$, is sent. The decision maker receives $\nabla f_{\tau_i^s}(\cdot)$ after some delay that can last for multiple time slots. Any feedback received after the next decision $\mathbf{x}_{i+1}$ is assumed to be dropped. Due to random delays, the gradient feedbacks may be received out of order.

Besides $\mathcal{X}_0$, we also consider long-term constraints on $\{\mathbf{x}_t\}$, which arise in many practical applications as explained in Section I. Let $\mathbf{g}(\mathbf{x}) = [g^1(\mathbf{x}), \ldots, g^C(\mathbf{x})]^T : \mathbb{R}^n \to \mathbb{R}^C$ be a vector of C constraint functions. The decision sequence is subject to long-term constraints $\sum_{t \in \mathcal{T}} \mathbf{g}(\mathbf{x}_t) \preceq \mathbf{0}$. With periodic decision updates, it is equivalent to satisfying $\sum_{i \in \mathcal{I}} T_i \mathbf{g}(\mathbf{x}_i) \preceq \mathbf{0}$.

Thus, the goal of constrained OCO with periodic updates is to select a sequence of decisions $\{\mathbf{x}_i\}$, for $\mathbf{x}_i \in \mathcal{X}_0$, to minimize the accumulated loss functions while meeting the long-term constraints. This leads to the following optimization problem:

$$\mathbf{P1}: \quad \min_{\{\mathbf{x}_i\}} \quad \sum_{i \in \mathcal{I}} \sum_{t \in \mathcal{T}_i} f_t(\mathbf{x}_i)$$

$$\text{s.t.} \quad \sum_{i \in \mathcal{I}} T_i \mathbf{g}(\mathbf{x}_i) \preceq \mathbf{0}, \tag{1}$$

$$\mathbf{x}_i \in \mathcal{X}_0, \quad \forall i \in \mathcal{I}. \tag{2}$$

Different from existing works on OCO with only short-term constraints [7], [10]-[17], the

additional long-term constraints in (1) of **P1** lead to a more complicated online optimization problem, especially since the underlying system varies over time while the online decision is fixed for a period. Note that in the special case when update period $T_i = 1$ for any $i \in \mathcal{I}$, **P1** is simplified to the standard constrained OCO problem with per-time-slot updates as in [18], [19], [22].

B. Performance Metric

Due to the lack of in-time information about the current loss functions under the OCO setting, an optimal solution to **P1** cannot be obtained.[1] We consider the following performance measurements typically adopted for developing the solution for constrained OCO, with a slight modification tailored to periodic updates.

We aim at designing a decision sequence $\{\mathbf{x}_i\}$ over update periods, such that the accumulated loss in the objective of **P1** is competitive with some benchmark under the same set of gradient feedbacks. Thus, for the static regret, we consider the following static offline benchmark, which is generalized from the per-time-slot one used in [18]-[20], [22], [23] to accommodate periodic updates:

$$\mathbf{x}^\star \triangleq \arg\min_{\mathbf{x}\in\mathcal{X}} \sum_{i\in\mathcal{I}} \frac{T_i}{S_i} \sum_{s\in\mathcal{S}_i} f_{\tau_i^s}(\mathbf{x}) \tag{3}$$

where $\mathcal{X} \triangleq \{\mathbf{x} \in \mathcal{X}_0 : \mathbf{g}(\mathbf{x}) \preceq \mathbf{0}\}$. Note that $\mathbf{x}^\star$ is computed offline assuming all the loss functions $f_{\tau_i^s}(\mathbf{x})$, for all $s \in \mathcal{S}_i$ and $i \in \mathcal{I}$, are known in advance. Then, the static regret is the performance gap between $\{\mathbf{x}_i\}$ and $\mathbf{x}^\star$:

$$\mathrm{RE_s}(T) \triangleq \sum_{i\in\mathcal{I}} \frac{T_i}{S_i} \sum_{s\in\mathcal{S}_i} \left(f_{\tau_i^s}(\mathbf{x}_i) - f_{\tau_i^s}(\mathbf{x}^\star)\right). \tag{4}$$

However, the static regret only provides a coarse performance measure when the underlying system is time-varying and may not be an attractive metric to use. A more useful performance benchmark is the dynamic benchmark $\{\mathbf{x}_i^\circ\}$, given by

$$\mathbf{x}_i^\circ \triangleq \arg\min_{\mathbf{x}\in\mathcal{X}} \frac{T_i}{S_i} \sum_{s\in\mathcal{S}_i} f_{\tau_i^s}(\mathbf{x}). \tag{5}$$

[1]In fact, even for the simplest original OCO problem [7] (*i.e.,* under the per-time-slot update setting without long-term constraints (1)), an optimal solution cannot be found [10].

For the case of per-time-slot updates, the dynamic benchmark was originally proposed for OCO with short-term constraints [7] and was modified in [21], [24], [25] to incorporate long-term constraints. Here, we generalize it to account for periodic updates. In (5), $\mathbf{x}_i^\circ$ is computed using all the S_i loss functions $f_{\tau_i^s}(\mathbf{x})$ in the current update period i. Then, the dynamic regret is

$$\mathrm{RE_d}(T) \triangleq \sum_{i\in\mathcal{I}} \frac{T_i}{S_i} \sum_{s\in\mathcal{S}_i} \left(f_{\tau_i^s}(\mathbf{x}_i) - f_{\tau_i^s}(\mathbf{x}_i^\circ)\right). \tag{6}$$

The gap between the static and dynamic regrets can be as large as $\mathcal{O}(T)$ [31]. In this paper, for comprehensive performance analysis, we provide upper bounds for both $\mathrm{RE_s}(T)$ and $\mathrm{RE_d}(T)$.

Remark 1. Note that with incomplete gradient feedbacks, *i.e.,* $\sum_{i\in\mathcal{I}} S_i = S < T$, our regret definitions in (4) and (6) fully utilize the feedback information. Our accumulated loss in each period i is the average loss over time slots when the gradient feedbacks are provided, *i.e.,* $\frac{1}{S_i}\sum_{s\in\mathcal{S}_i} f_{\tau_i^s}(\mathbf{x}_i)$, scaled by the duration T_i of the update period i, for $i \in \mathcal{I}$. If the environment is mean stationary, *i.e.,* $\mathbb{E}\{f_t(\mathbf{x})\} = \mathbb{E}\{f_{t'}(\mathbf{x})\}$ for any $t, t' \in \mathcal{T}$, then in the expectation sense, the accumulated loss in our regret definitions is the same as the actual loss in the objective of **P1**, *i.e.,*

$$\mathbb{E}\left\{\sum_{i\in\mathcal{I}} \frac{T_i}{S_i} \sum_{s\in\mathcal{S}_i} \left(f_{\tau_i^s}(\mathbf{x}_i)\right)\right\} = \mathbb{E}\left\{\sum_{i\in\mathcal{I}} \sum_{t\in\mathcal{T}_i} \left(f_t(\mathbf{x}_i)\right)\right\}.$$

More generally, suppose there exists a constant $d > 0$ such that $|f_t(\mathbf{x}) - f_{t'}(\mathbf{x})| \leq d$, for any $\mathbf{x} \in \mathcal{X}_0$ and $t, t' \in \mathcal{T}_i$, $i \in \mathcal{I}$. Then, we have $\sum_{i\in\mathcal{I}} \frac{T_i}{S_i} \sum_{s\in\mathcal{S}_i} (f_{\tau_i^s}(\mathbf{x}_i)) - \sum_{i\in\mathcal{I}} \sum_{t\in\mathcal{T}_i} (f_t(\mathbf{x}_i)) = \mathcal{O}(d(T-S))$. This performance gap can be small if the system does not fluctuate too much over time. Furthermore, it approaches zero as the number of feedbacks $S \to T$.

We also need to measure the accumulated violation of each long-term constraint $c \in \mathcal{C} = \{1, \ldots, C\}$. Define the constraint violation as

$$\mathrm{VO}^c(T) \triangleq \sum_{i\in\mathcal{I}} T_i g^c(\mathbf{x}_i), \quad \forall c \in \mathcal{C}. \tag{7}$$

Note that the constraint violation defined in [18]-[25] are under the standard per-time-slot update setting. In contrast, our model accommodates the possibly time-varying update periods of multiple time slots.

IV. The Periodic Queueing and Gradient Aggregation (PQGA) Algorithm

In this section, we present an efficient algorithm, PQGA, to solve the formulated constrained OCO problem. It uses a periodic virtual queue and periodic updates after solving per-period optimization problems that are convex and hence practically solvable. We further show that, despite its low implementation complexity, PQGA provides provable performance guarantees in terms of dynamic regret, static regret, and constraint violation bounds.

A. PQGA Algorithm Description

PQGA introduces a *periodic* virtual queue vector $\mathbf{Q}_i = [Q_i^1, \ldots, Q_i^C]^T$ in each update period $i \in \mathcal{I}$, with the following updating rule:

$$Q_{i+1}^c = \max\{-\gamma T_i g^c(\mathbf{x}_i), Q_i^c + \gamma T_i g^c(\mathbf{x}_i)\}, \quad \forall c \in \mathcal{C} \tag{8}$$

where $\gamma > 0$ is an algorithm parameter. The role of $\mathbf{Q}_i$ is similar to a Lagrange multiplier vector for the long-term constraints in (1), and the value of $\mathbf{Q}_i$ reflects the accumulated violation of the long-term constraints. We remark here that (8) is different from the virtual queues used in the standard Lyapunov optimization [26] and subsequent extensions to OCO [22]-[25]. Unique to our proposed approach, $T_i g^c(\mathbf{x}_i)$ is the accumulated constraint violation in update period i, and it is scaled by an appropriate factor γ.

In the basic form of PQGA, instead of solving **P1** directly, we solve a *per-period* problem at the beginning of each update period $i+1$ with the short-term constraints only, given by

$$\mathbf{P2}: \min_{\mathbf{x}\in\mathcal{X}_0} \frac{T_i}{S_i} \sum_{s\in\mathcal{S}_i} [\nabla f_{\tau_i^s}(\mathbf{x}_i)]^T(\mathbf{x}-\mathbf{x}_i) + \alpha\|\mathbf{x}-\mathbf{x}_i\|^2 + [\mathbf{Q}_{i+1} + \gamma T_i \mathbf{g}(\mathbf{x}_i)]^T[\gamma T_{i+1}\mathbf{g}(\mathbf{x})]$$

where $\alpha, \gamma > 0$ are two algorithm parameters. In **P2**, the gradient direction is aggregated based on all the gradient feedbacks $\{\nabla f_{\tau_i^s}(\cdot), s \in \mathcal{S}_i\}$, collected in the previous update period i. The regularization term $\alpha\|\mathbf{x}-\mathbf{x}_i\|^2$ controls how much the new decision $\mathbf{x}_{i+1}$ is allowed to change from the previous decision $\mathbf{x}_i$. Furthermore, in the last term of the objective function of **P2**, we consider an inner-product between the vector of periodic queue lengths and the period-weighted vector of the long-term constraint functions, which represents a penalty of constraint violation in $\mathbf{g}(\mathbf{x})$. Thus, we convert the long-term constraints in (1) to a penalty term on $\mathbf{g}(\mathbf{x})$ as one part of the objective function in **P2**.

In addition to the basic form of PQGA that uses a single step of gradient descent in **P2**, we can further configure PQGA to incorporate multi-step gradient descent. Multi-step gradient descent has previously been shown to provide stronger optimization results for OCO with short-term constraints [16]. In this work, we will further verify that it also provides performance improvement to PQGA under both short-term and long-term constraints. Specifically, at the beginning of each update period $i+1$, after updating the periodic virtual queue in (8), we initialize an intermediate decision vector $\tilde{\mathbf{x}}_i^0 = \mathbf{x}_i$. We then perform J-step aggregated gradient descent to generate $\tilde{\mathbf{x}}_i^J$ for any $J \geq 0$. If $J = 0$, we readily have $\tilde{\mathbf{x}}_i^J = \mathbf{x}_i$ by initialization. Otherwise, for each gradient descent step $j \in \mathcal{J} = \{1, \ldots, J\}$, we solve the following optimization problem for $\tilde{\mathbf{x}}_i^j$:

$$\min_{\mathbf{x}\in\mathcal{X}_0} \ \frac{T_i}{S_i}\sum_{s\in\mathcal{S}_i}[\nabla f_{\tau_i^s}(\tilde{\mathbf{x}}_i^{j-1})]^T(\mathbf{x}-\tilde{\mathbf{x}}_i^{j-1}) + \alpha\|\mathbf{x}-\tilde{\mathbf{x}}_i^{j-1}\|^2.$$

The above problem is similar to the standard projected gradient descent problem. Therefore, its solution is readily available:

$$\tilde{\mathbf{x}}_i^j = \mathcal{P}_{\mathcal{X}_0}\left\{\tilde{\mathbf{x}}_i^{j-1} - \frac{1}{2\alpha}\left(\frac{T_i}{S_i}\sum_{s\in\mathcal{S}_i}\nabla f_{\tau_i^s}(\tilde{\mathbf{x}}_i^{j-1})\right)\right\} \tag{9}$$

where $\mathcal{P}_{\mathcal{X}_0}\{\mathbf{x}\} \triangleq \arg\min_{\mathbf{y}\in\mathcal{X}_0}\{\|\mathbf{y}-\mathbf{x}\|^2\}$ is the projection operator onto the convex feasible set $\mathcal{X}_0$ and α can be viewed as a step-size parameter.

With both $\mathbf{x}_i$ and $\tilde{\mathbf{x}}_i^J$, we then modify **P2** to the following per-period optimization problem for $\mathbf{x}_{i+1}$:

$$\textbf{P2}': \min_{\mathbf{x}\in\mathcal{X}_0} \frac{T_i}{S_i}\sum_{s\in\mathcal{S}_i}[\nabla f_{\tau_i^s}(\tilde{\mathbf{x}}_i^J)]^T(\mathbf{x}-\tilde{\mathbf{x}}_i^J)+\alpha\|\mathbf{x}-\tilde{\mathbf{x}}_i^J\|^2+\eta\|\mathbf{x}-\mathbf{x}_i\|^2+[\mathbf{Q}_{i+1}+\gamma T_i\mathbf{g}(\mathbf{x}_i)]^T[\gamma T_{i+1}\mathbf{g}(\mathbf{x})]$$

where $\alpha, \eta, \gamma > 0$ and $J \geq 0$ are four algorithm parameters. Note that **P2′** uses double regularization on both $\mathbf{x}_i$ and $\tilde{\mathbf{x}}_i^J$. The intuition behind the double regularization is that both $\mathbf{x}_i$ and $\tilde{\mathbf{x}}_i^J$ help to minimize the accumulate loss and constraint violation. Therefore, it is beneficial to prevent the new decision $\mathbf{x}_{i+1}$ from being too far away from either of them. This will be shown, analytically in Section IV-B, to give PQGA substantial performance advantage over existing works in terms of performance bounds.

The PQGA algorithm is given in Algorithm 1. Note that PQGA has four algorithm parameters α, η, γ, and J. We will discuss the choice of their values in Section IV-C, after we derive the

Algorithm 1 The PQGA Algorithm

Initialization: $\alpha, \eta, \gamma > 0$, $J \geq 0$, $\mathbf{x}_0 \in \mathcal{X}_0$, and $\mathbf{Q}_0 = \mathbf{0}$.
At the beginning of each update period $i+1$, do:
  Update the periodic virtual queue $\mathbf{Q}_{i+1}$ via (8).
  Initialize the intermediate decision vector $\tilde{\mathbf{x}}_i^0 = \mathbf{x}_i$.
  for $j = 1$ **to** J
    Update $\tilde{\mathbf{x}}^j$ via (9).
  end for
  Update the periodic decision $\mathbf{x}_{i+1}$ by solving **P2′** using $\mathbf{Q}_{i+1}$, $\mathbf{x}_i$, and $\tilde{\mathbf{x}}^J$.

regret and constraint violation bounds, to explain the impact of these four parameters on those bounds. During each update period $i \in \mathcal{I}$, the decision maker collects the delayed and possibly incomplete gradient information $\nabla f_{\tau_i^s}(\cdot), s \in \mathcal{S}_i$. At the beginning of the next update period $i+1$, it first updates the periodic virtual queue $\mathbf{Q}_{i+1}$ in (8) based on the accumulated constraint violation caused by its previous decision $\mathbf{x}_i$. It then learns the gradient descent direction from the collected past gradient information and performs J-step aggregated gradient descent to generate $\tilde{\mathbf{x}}^J$. Finally, it weights the constraint functions based on the updated queue lengths and regularizes on both $\tilde{\mathbf{x}}^J$ and $\mathbf{x}_i$, to compute the decision $\mathbf{x}_{i+1}$ for update period $i+1$ by solving **P2′**.[2]

Remark 2. **P2** and **P2′** are strongly convex optimization problems, so they can be solved efficiently using well-known optimization tools. Furthermore, as shown in Section V-B, for the considered problem of precoding-based massive MIMO virtualization, it has a closed-form solution with negligible computational complexity.

Remark 3. When the vector long-term constraint function $\mathbf{g}(\mathbf{x})$ is separable w.r.t. $\mathbf{x}$, **P2** and **P2′** can be equivalently decomposed into independent subproblems. In this case, PQGA can be implemented distributively with even lower computational complexity.

B. Regret and Constraint Violation Bounds of PQGA

Existing analysis techniques for the standard per-time-slot OCO setting with single-step gradient descent [18]-[25] are inadequate for studying the performance of PQGA. In this section, we present new techniques to derive the regret and constraint violation bounds of PQGA, particularly

[2]When $J = 0$, we readily have $\tilde{\mathbf{x}}^J = \mathbf{x}_i$ by initialization. In this case, the double regularization in **P2′** on $\tilde{\mathbf{x}}^J$ and $\mathbf{x}_i$ can be combined as a single regularization on $\mathbf{x}_i$, and **P2′** is equivalent to **P2**.

to account for the periodic queues and possibly multi-step aggregated gradient descent. Although a small part of our derivations uses techniques from Lyapunov drift analysis, as explained in Section II, PQGA is structurally different from Lyapunov optimization.

We make the following assumptions that are common in the literature of OCO.

Assumption 1. For any t, the loss function $f_t(\mathbf{x})$ satisfies the following:

1.1) $f_t(\mathbf{x})$ is 2ϱ-strongly convex over $\mathcal{X}_0$: $\exists\ \varrho > 0$, s.t., for any $\mathbf{x}, \mathbf{y} \in \mathcal{X}_0$ and t

$$f_t(\mathbf{y}) \geq f_t(\mathbf{x}) + [\nabla f_t(\mathbf{x})]^T(\mathbf{y} - \mathbf{x}) + \varrho\|\mathbf{y} - \mathbf{x}\|^2. \tag{10}$$

1.2) $f_t(\mathbf{x})$ is $2L$-smooth over $\mathcal{X}_0$: $\exists\ L > 0$, s.t., for any $\mathbf{x}, \mathbf{y} \in \mathcal{X}_0$ and t

$$f_t(\mathbf{y}) \leq f_t(\mathbf{x}) + [\nabla f_t(\mathbf{x})]^T(\mathbf{y} - \mathbf{x}) + L\|\mathbf{y} - \mathbf{x}\|^2. \tag{11}$$

Assumption 2. The gradient $\nabla f_t(\mathbf{x})$ is bounded: $\exists\ D > 0$, s.t.,

$$\|\nabla f_t(\mathbf{x})\| \leq D, \quad \forall \mathbf{x} \in \mathcal{X}_0, \quad \forall t \in \mathcal{T}. \tag{12}$$

Assumption 3. The long-term constraint functions satisfy the following:

3.1) $\mathbf{g}(\mathbf{x})$ is Lipschitz continuous on $\mathcal{X}_0$: $\exists\ \beta > 0$, s.t.,

$$\|\mathbf{g}(\mathbf{x}) - \mathbf{g}(\mathbf{y})\| \leq \beta\|\mathbf{x} - \mathbf{y}\|, \quad \forall \mathbf{x}, \mathbf{y} \in \mathcal{X}_0. \tag{13}$$

3.2) $\mathbf{g}(\mathbf{x})$ is bounded: $\exists\ G > 0$, s.t.,

$$\|\mathbf{g}(\mathbf{x})\| \leq G, \quad \forall \mathbf{x} \in \mathcal{X}_0. \tag{14}$$

3.3) Existence of an interior point: $\exists\ \epsilon > 0$ and $\mathbf{x}' \in \mathcal{X}_0$, s.t.,

$$\mathbf{g}(\mathbf{x}') \preceq -\epsilon\mathbf{1}. \tag{15}$$

Assumption 4. The radius of $\mathcal{X}_0$ is bounded: $\exists\ R > 0$, s.t.,

$$\|\mathbf{x} - \mathbf{y}\| \leq R, \quad \forall \mathbf{x}, \mathbf{y} \in \mathcal{X}_0. \tag{16}$$

Remark 4. Strongly convex loss functions arise in many machine learning and signal processing applications, such as Lasso regression, support vector machine, softmax classifier, and robust subspace tracking. Furthermore, for applications with general convex loss functions, it is common

to add a simple regularization term such as $\mu\|\mathbf{x}\|^2$, so that the overall optimization objective becomes strongly convex [17].

1) Bounding the Dynamic Regret: A main goal of this paper is to examine the impact of possibly time-varying update periods and multi-step aggregated gradient descent on the dynamic regret bound for constrained OCO, which has not been addressed in the existing literature. To this end, we define the accumulated variation of the dynamic benchmark $\{\mathbf{x}_i^\circ\}$ (termed the path length in [7]) as

$$\Pi_{\mathbf{x}^\circ} \triangleq \sum_{i\in\mathcal{I}} \|\mathbf{x}_i^\circ - \mathbf{x}_{i+1}^\circ\|. \tag{17}$$

Another related quantity regarding the accumulated variation of the time-varying update periods $\{T_i\}$ is defined as

$$\Pi_T \triangleq \sum_{i\in\mathcal{I}} (T_i - T_{i+1})^2. \tag{18}$$

We first provide bounds on the periodic virtual queues $\{\mathbf{Q}_i\}$ produced by PQGA in the following lemma.

Lemma 1. The following statements hold for any $i \in \mathcal{I}$:

$$\mathbf{Q}_i \succeq \mathbf{0}, \tag{19}$$

$$\mathbf{Q}_{i+1} + \gamma T_i \mathbf{g}(\mathbf{x}_i) \succeq \mathbf{0}, \tag{20}$$

$$\|\mathbf{Q}_{i+1}\| \geq \|\gamma T_i \mathbf{g}(\mathbf{x}_i)\|, \tag{21}$$

$$\|\mathbf{Q}_{i+1}\| \leq \|\mathbf{Q}_i\| + \|\gamma T_i \mathbf{g}(\mathbf{x}_i)\|. \tag{22}$$

Proof: The periodic virtual queue vector is initialized as $\mathbf{Q}_0 = \mathbf{0}$. For any $c \in \mathcal{C}$ and $i \in \mathcal{I}$, by induction, we first assume $Q_i^c \geq 0$. From the periodic virtual queue dynamics in (8), if $\gamma T_i g^c(\mathbf{x}_i) \geq 0$, then $Q_{i+1}^c \geq Q_i^c + \gamma T_i g^c(\mathbf{x}_i) \geq 0$; otherwise, we have $Q_{i+1}^c \geq -\gamma T_i g^c(\mathbf{x}_i) \geq 0$. Combining the above two cases, we have (19).

From (8), for any $c \in \mathcal{C}$ and $i \in \mathcal{I}$, we have $Q_{t+1}^c \geq -\gamma T_i g^c(\mathbf{x}_i)$, which yields (20).

For any $c \in \mathcal{C}$ and $i \in \mathcal{I}$, from (8) and $Q_i^c \geq 0$ in (19), if $\gamma T_i g^c(\mathbf{x}_i) \geq 0$, then $Q_{i+1}^c \geq Q_i^c + \gamma T_i g^c(\mathbf{x}_i) \geq \gamma T_i g^c(\mathbf{x}_i)$; otherwise, we have $Q_{i+1}^c \geq -\gamma T_i g^c(\mathbf{x}_i)$. Therefore, we have $Q_{i+1}^c \geq |\gamma T_i g^c(\mathbf{x}_i)|$. Squaring both sides and summing over $c \in \mathcal{C}$ yields (21).

From (8), for any $c \in \mathcal{C}$ and $i \in \mathcal{I}$, we have $Q_{i+1}^c \leq Q_i^c + |\gamma T_i g^c(\mathbf{x}_i)|$. Since $Q_i^c \geq 0$ in (19), by the triangle inequality, we have $\|\mathbf{Q}_{i+1}\| \leq \sqrt{\sum_{c\in\mathcal{C}}(Q_i^c + |\gamma T_i g^c(\mathbf{x}_i)|)^2} \leq \|\mathbf{Q}_i\| + \|\gamma T_i \mathbf{g}(\mathbf{x}_i)\|$, which yields (22). ■

Define $L_i \triangleq \frac{1}{2}\|\mathbf{Q}_i\|^2$ as the quadratic Lyapunov function and $\Delta_i \triangleq L_{i+1} - L_i$ as the Lyapunov drift for each update period $i \in \mathcal{I}$. Leveraging the results in Lemma 1, we provide an upper bound on the Lyapunov drift Δ_i in the following lemma.

Lemma 2. The Lyapunov drift is upper bounded for any $i \in \mathcal{I}$ as follows:

$$\Delta_i \leq \mathbf{Q}_i^T[\gamma T_i \mathbf{g}(\mathbf{x}_i)] + \|\gamma T_i \mathbf{g}(\mathbf{x}_i)\|^2. \tag{23}$$

Proof: For any $c \in \mathcal{C}$ and $i \in \mathcal{I}$, we first prove

$$\frac{1}{2}(Q_{i+1}^c)^2 - \frac{1}{2}(Q_i^c)^2 \leq Q_i^c[\gamma T_i g^c(\mathbf{x}_i)] + [\gamma T_i g^c(\mathbf{x}_i)]^2 \tag{24}$$

by considering the following two cases.

1) $Q_i^c + \gamma T_i g^c(\mathbf{x}_i) \geq -\gamma T_i g^c(\mathbf{x}_i)$*:* From the virtual queue dynamics in (8), we have $Q_{i+1}^c = Q_i^c + \gamma T_i g^c(\mathbf{x}_i)$. It then follows that

$$\frac{1}{2}(Q_{i+1}^c)^2 = \frac{1}{2}[Q_i^c + \gamma T_i g^c(\mathbf{x}_i)]^2 \leq \frac{1}{2}(Q_i^c)^2 + Q_i^c[\gamma T_i g^c(\mathbf{x}_i)] + [\gamma T_i g^c(\mathbf{x}_i)]^2.$$

2) $Q_i^c + \gamma T_i g^c(\mathbf{x}_i) < -\gamma T_i g^c(\mathbf{x}_i)$*:* We have $Q_{i+1}^c = -\gamma T_i g^c(\mathbf{x}_i)$ from (8). It then follows that

$$\frac{1}{2}(Q_{i+1}^c)^2 \leq \frac{1}{2}[\gamma T_i g^c(\mathbf{x}_i)]^2 + \frac{1}{2}[Q_i^c + \gamma T_i g^c(\mathbf{x}_i)]^2 = \frac{1}{2}(Q_i^c)^2 + Q_i^c[\gamma T_i g^c(\mathbf{x}_i)] + [\gamma T_i g^c(\mathbf{x}_i)]^2.$$

Combining the above two cases, we have (24). Summing (24) over $c \in \mathcal{C}$ yields (23). ■

We also require the following two lemmas, which are reproduced from Lemma 2.8 in [3] and Lemma 1 in [16], respectively.

Lemma 3. Let $\mathcal{Z} \subseteq \mathbb{R}^n$ be a nonempty convex set. Let $h(\mathbf{z}) : \mathbb{R}^n \to \mathbb{R}$ be a 2ς-strongly-convex function over $\mathcal{Z}$ w.r.t. $\|\cdot\|$. Let $\mathbf{w} = \arg\min_{\mathbf{z}\in\mathcal{Z}}\{h(\mathbf{z})\}$. Then, for any $\mathbf{u} \in \mathcal{Z}$, we have $h(\mathbf{w}) \leq h(\mathbf{u}) - \varsigma\|\mathbf{u} - \mathbf{w}\|^2$.

Lemma 4. Let $\mathcal{Z} \subseteq \mathbb{R}^n$ be a nonempty convex set. Let $h(\mathbf{z}) : \mathbb{R}^n \to \mathbb{R}$ be a 2ς-strongly-convex and 2ζ-smooth function over $\mathcal{Z}$ w.r.t. $\|\cdot\|$. Let $\mathbf{v} = \arg\min_{\mathbf{z}\in\mathcal{Z}}\{[\nabla h(\mathbf{u})]^T(\mathbf{z} - \mathbf{u}) + \upsilon\|\mathbf{z} - \mathbf{u}\|^2\}$ and $\mathbf{w} = \arg\min_{\mathbf{z}\in\mathcal{Z}}\{h(\mathbf{z})\}$. Then, for any $\upsilon \geq \zeta$, we have $\|\mathbf{w} - \mathbf{v}\|^2 \leq \frac{\upsilon-\varsigma}{\upsilon+\varsigma}\|\mathbf{w} - \mathbf{u}\|^2$.

Based on Lemmas 1-4, for any number of aggregated gradient descent steps $J \geq 0$, we provide an upper bound on the dynamic regret $\mathrm{RE_d}(T)$ for PQGA in the following theorem.

Theorem 1. For any $J \geq 0$, if we choose $\alpha \geq T_{\max} L$, $\eta \geq \beta^2\gamma^2 T_{\max}^2$, and $\gamma > 0$, the dynamic regret of PQGA is upper bounded by

$$\mathrm{RE_d}(T) \leq \frac{D^2 T_{\max}}{4\alpha} T + (\alpha\rho^J + \eta)(R^2 + 2R\Pi_{\mathbf{x}^\circ}) + \gamma^2 G^2 (T_{\max}^2 + \Pi_T) \tag{25}$$

where $\rho = \frac{\alpha - \varrho}{\alpha + \varrho} < 1$.

Proof: The objective function of **P2′** is $2(\alpha+\eta)$-strongly convex over $\mathcal{X}_0$ w.r.t. $\|\cdot\|$ due to the double regularization. Since $\mathbf{x}_{i+1}$ minimizes **P2′** over $\mathcal{X}_0$ for any $i \in \mathcal{I}$, we have

$$\begin{aligned}
&\frac{T_i}{S_i}\sum_{s\in\mathcal{S}_i}[\nabla f_{\tau_i^s}(\tilde{\mathbf{x}}_i^J)]^T(\mathbf{x}_{i+1}-\tilde{\mathbf{x}}_i^J) + \alpha\|\mathbf{x}_{i+1}-\tilde{\mathbf{x}}_i^J\|^2 + [\mathbf{Q}_{i+1}+\gamma T_i \mathbf{g}(\mathbf{x}_i)]^T[\gamma T_{i+1}\mathbf{g}(\mathbf{x}_{i+1})] + \eta\|\mathbf{x}_{i+1}-\mathbf{x}_i\|^2 \\
&\overset{(a)}{\leq} \frac{T_i}{S_i}\sum_{s\in\mathcal{S}_i}[\nabla f_{\tau_i^s}(\tilde{\mathbf{x}}_i^J)]^T(\mathbf{x}_i^\circ-\tilde{\mathbf{x}}_i^J) + \alpha\|\mathbf{x}_i^\circ-\tilde{\mathbf{x}}_i^J\|^2 + [\mathbf{Q}_{i+1}+\gamma T_i \mathbf{g}(\mathbf{x}_i)]^T[\gamma T_{i+1}\mathbf{g}(\mathbf{x}_i^\circ)] + \eta\|\mathbf{x}_i^\circ-\mathbf{x}_i\|^2 \\
&\quad - (\alpha+\eta)\|\mathbf{x}_i^\circ-\mathbf{x}_{i+1}\|^2 \\
&\overset{(b)}{\leq} \frac{T_i}{S_i}\sum_{s\in\mathcal{S}_i}[\nabla f_{\tau_i^s}(\tilde{\mathbf{x}}_i^J)]^T(\mathbf{x}_i^\circ-\tilde{\mathbf{x}}_i^J) + \alpha(\|\mathbf{x}_i^\circ-\tilde{\mathbf{x}}_i^J\|^2 - \|\mathbf{x}_i^\circ-\mathbf{x}_{i+1}\|^2) + \eta(\|\mathbf{x}_i^\circ-\mathbf{x}_i\|^2 - \|\mathbf{x}_i^\circ-\mathbf{x}_{i+1}\|^2)
\end{aligned} \tag{26}$$

where (a) follows from Lemma 3, and (b) is because $\mathbf{Q}_{i+1}+\gamma T_i \mathbf{g}(\mathbf{x}_i) \succeq \mathbf{0}$ in (20) and $\mathbf{g}(\mathbf{x}_i^\circ) \preceq \mathbf{0}$ in (3) such that $[\mathbf{Q}_{i+1}+\gamma T_i \mathbf{g}(\mathbf{x}_i)]^T[\gamma T_{i+1}\mathbf{g}(\mathbf{x}_i^\circ)] \preceq \mathbf{0}$ for any $i \in \mathcal{I}$.

We now bound the RHS of (26). Note that the aggregated loss function $\frac{T_i}{S_i}\sum_{s\in\mathcal{S}_i} f_{\tau_i^s}(\mathbf{x})$ is $T_i\varrho$-strongly convex for any $i \in \mathcal{I}$. Applying Lemma 4 to the update of $\tilde{\mathbf{x}}_i^j$ in (9), for any $\alpha \geq T_i L$, we have

$$\|\mathbf{x}_i^\circ - \tilde{\mathbf{x}}_i^j\|^2 \leq \frac{\alpha - T_i\varrho}{\alpha + T_i\varrho}\|\mathbf{x}_i^\circ - \tilde{\mathbf{x}}_i^{j-1}\|^2, \quad \forall j \in \mathcal{J}.$$

Note that the strong convexity constant ϱ is smaller than the constant of gradient Lipschitz continuity, *i.e.,* $\varrho \leq L$ [15]. Combining the above J inequalities and noting that $\tilde{\mathbf{x}}_i^0 = \mathbf{x}_i$ by initialization, $1 \leq T_i \leq T_{\max}$, and $\alpha \geq T_{\max} L$ such that $\frac{\alpha - T_i\varrho}{\alpha + T_i\varrho} \leq \rho = \frac{\alpha-\varrho}{\alpha+\varrho}$, we have

$$\|\mathbf{x}_i^\circ - \tilde{\mathbf{x}}_i^J\|^2 \leq \rho^J \|\mathbf{x}_i^\circ - \mathbf{x}_i\|^2. \tag{27}$$

Also, from $\|\mathbf{a}+\mathbf{b}\|^2 \geq \|\mathbf{a}\|^2 + \|\mathbf{b}\|^2 - 2\|\mathbf{a}\|\|\mathbf{b}\|$ and the bound on $\mathcal{X}_0$ in (16), we have

$$\begin{aligned}
&\|\mathbf{x}_i^\circ - \mathbf{x}_i\|^2 - \|\mathbf{x}_i^\circ - \mathbf{x}_{i+1}\|^2 \\
&\quad \leq \|\mathbf{x}_i^\circ - \mathbf{x}_i\|^2 - \|\mathbf{x}_{i+1}^\circ - \mathbf{x}_{i+1}\|^2 - \|\mathbf{x}_{i+1}^\circ - \mathbf{x}_i^\circ\|^2 + 2\|\mathbf{x}_{i+1}^\circ - \mathbf{x}_{i+1}\|\|\mathbf{x}_{i+1}^\circ - \mathbf{x}_i^\circ\| \leq \Psi_i + 2R\psi_i
\end{aligned} \tag{28}$$

where we define $\Psi_i \triangleq \|\mathbf{x}_i^\circ - \mathbf{x}_i\|^2 - \|\mathbf{x}_{i+1}^\circ - \mathbf{x}_{i+1}\|^2$ and $\psi_i \triangleq \|\mathbf{x}_i^\circ - \mathbf{x}_{i+1}^\circ\|$.

Substituting (27) and (28) into (26), we have

$$\frac{T_i}{S_i}\sum_{s\in\mathcal{S}_i}[\nabla f_{\tau_i^s}(\tilde{\mathbf{x}}_i^J)]^T(\mathbf{x}_{i+1}-\tilde{\mathbf{x}}_i^J)+\alpha\|\mathbf{x}_{i+1}-\tilde{\mathbf{x}}_i^J\|^2+[\mathbf{Q}_{i+1}+\gamma T_i\mathbf{g}(\mathbf{x}_i)]^T[\gamma T_{i+1}\mathbf{g}(\mathbf{x}_{i+1})]+\eta\|\mathbf{x}_{i+1}-\mathbf{x}_i\|^2$$
$$\leq \frac{T_i}{S_i}\sum_{s\in\mathcal{S}_i}[\nabla f_{\tau_i^s}(\mathbf{x}_i)]^T(\mathbf{x}_i^\circ-\mathbf{x}_i)+(\alpha\rho^J+\eta)(\Psi_i+2R\psi_i). \tag{29}$$

Adding $\frac{T_i}{S_i}\sum_{s\in\mathcal{S}_i} f_{\tau_i^s}(\mathbf{x}_i)$ on both sides of (29), noting that $f_{\tau_i^s}(\mathbf{x}_i)+[\nabla f_{\tau_i^s}(\mathbf{x}_i)]^T(\mathbf{x}_i^\circ-\mathbf{x}_i)\leq f_{\tau_i^s}(\mathbf{x}_i^\circ)$ from the convexity of $f_{\tau_i^s}(\mathbf{x})$ for any $s\in\mathcal{S}_i$, and rearranging terms, we have

$$\frac{T_i}{S_i}\sum_{s\in\mathcal{S}_i}\left[f_{\tau_i^s}(\mathbf{x}_i)-f_{\tau_i^s}(\mathbf{x}_i^\circ)\right]$$
$$\leq -\frac{T_i}{S_i}\sum_{s\in\mathcal{S}_i}[\nabla f_{\tau_i^s}(\tilde{\mathbf{x}}_i^J)]^T(\mathbf{x}_{i+1}-\tilde{\mathbf{x}}_i^J)-\alpha\|\mathbf{x}_{i+1}-\tilde{\mathbf{x}}_i^J\|^2-[\mathbf{Q}_{i+1}+\gamma T_i\mathbf{g}(\mathbf{x}_i)]^T[\gamma T_{i+1}\mathbf{g}(\mathbf{x}_{i+1})]$$
$$-\eta\|\mathbf{x}_{i+1}-\mathbf{x}_i\|^2+(\alpha\rho^J+\eta)(\Psi_i+2R\psi_i). \tag{30}$$

We then bound the RHS of (30). Completing the square, we have

$$-\frac{T_i}{S_i}\sum_{s\in\mathcal{S}_i}[\nabla f_{\tau_i^s}(\tilde{\mathbf{x}}_i^J)]^T(\mathbf{x}_{i+1}-\tilde{\mathbf{x}}_i^J)-\alpha\|\mathbf{x}_{i+1}-\tilde{\mathbf{x}}_i^J\|^2$$
$$=-\frac{T_i}{S_i}\sum_{s\in\mathcal{S}_i}\left(\left\|\frac{\nabla f_{\tau_i^s}(\tilde{\mathbf{x}}_i^J)}{2\sqrt{\frac{\alpha}{T_i}}}+\sqrt{\frac{\alpha}{T_i}}(\mathbf{x}_{i+1}-\tilde{\mathbf{x}}_i^J)\right\|^2-\frac{T_i\left\|\nabla f_{\tau_i^s}(\mathbf{x}_i)\right\|^2}{4\alpha}\right)\overset{(a)}{\leq}\frac{D^2T_{\max}}{4\alpha}T_i. \tag{31}$$

where (a) follows by noting that $\nabla f_t(\mathbf{x})$ is bounded in (12).

Also, note that

$$-[\mathbf{Q}_{i+1}+\gamma T_i\mathbf{g}(\mathbf{x}_i)]^T[\gamma\mathbf{g}T_{i+1}(\mathbf{x}_{i+1})]$$
$$\overset{(a)}{\leq}-\Delta_{i+1}+\|\gamma T_{i+1}\mathbf{g}(\mathbf{x}_{i+1})\|^2-[\gamma T_i\mathbf{g}(\mathbf{x}_i)]^T[\gamma T_{i+1}\mathbf{g}(\mathbf{x}_{i+1})]$$
$$\overset{(b)}{=}-\Delta_{i+1}+\frac{\gamma^2}{2}\|T_{i+1}\mathbf{g}(\mathbf{x}_{i+1})\|^2-\frac{\gamma^2}{2}\|T_i\mathbf{g}(\mathbf{x}_i)\|^2+\frac{\gamma^2}{2}\|T_i\mathbf{g}(\mathbf{x}_i)-T_{i+1}\mathbf{g}(\mathbf{x}_{i+1})\|^2$$
$$\overset{(c)}{\leq}-\Delta_{i+1}+\frac{\gamma^2}{2}\Phi_i+\beta^2\gamma^2T_i^2\|\mathbf{x}_{i+1}-\mathbf{x}_i\|^2+\gamma^2G^2(T_i-T_{i+1})^2 \tag{32}$$

where (a) follows from rearranging terms of (23) in Lemma 2 such that $-\mathbf{Q}_{i+1}^T[\gamma T_{i+1}\mathbf{g}(\mathbf{x}_{i+1})]\leq -\Delta_{i+1}+\|\gamma T_{i+1}\mathbf{g}(\mathbf{x}_{i+1})\|^2$, (b) is because $\mathbf{a}^T\mathbf{b}=\frac{1}{2}(\|\mathbf{a}\|^2+\|\mathbf{b}\|^2-\|\mathbf{a}-\mathbf{b}\|^2)$, and (c) follows from defining $\Phi_i\triangleq\|T_{i+1}\mathbf{g}(\mathbf{x}_{i+1})\|^2-\|T_i\mathbf{g}(\mathbf{x}_i)\|^2$, $\frac{1}{2}\|\mathbf{a}+\mathbf{b}\|^2\leq\|\mathbf{a}\|^2+\|\mathbf{b}\|^2$, and $\mathbf{g}(\mathbf{x})$ being Lipschitz continuous in (13) and bounded in (14) such that

$$\frac{1}{2}\|T_i\mathbf{g}(\mathbf{x}_i)-T_{i+1}\mathbf{g}(\mathbf{x}_{i+1})\|^2$$
$$\leq\|T_i\mathbf{g}(\mathbf{x}_i)-T_i\mathbf{g}(\mathbf{x}_{i+1})\|^2+\|T_i\mathbf{g}(\mathbf{x}_{i+1})-T_{i+1}\mathbf{g}(\mathbf{x}_{i+1})\|^2\leq\beta^2T_i^2\|\mathbf{x}_i-\mathbf{x}_{i+1}\|^2+G^2(T_i-T_{i+1})^2.$$

Substituting (31) and (32) into (30), and noting that $\eta \geq \beta^2\gamma^2 T_{\max}^2$, we have

$$\frac{T_i}{S_i}\sum_{s\in\mathcal{S}_i}\left(f_{\tau_i^s}(\mathbf{x}_i)-f_{\tau_i^s}(\mathbf{x}_i^\circ)\right) \leq \frac{D^2 T_{\max}}{4\alpha}T_i + (\alpha\rho^J+\eta)(\Psi_i+2R\psi_i) - \Delta_{i+1} + \frac{\gamma^2}{2}\Phi_i + \gamma^2 G^2 (T_i - T_{i+1})^2. \quad (33)$$

Summing (33) over $i \in \mathcal{I}$, we have

$$\begin{aligned}
\mathrm{RE_d}(T) &= \sum_{i\in\mathcal{I}}\frac{T_i}{S_i}\sum_{s\in\mathcal{S}_i}\left(f_{\tau_i^s}(\mathbf{x}_i)-f_{\tau_i^s}(\mathbf{x}_i^\circ)\right)\\
&\overset{(a)}{\leq} \frac{D^2 T_{\max}}{4\alpha}T + (\alpha\rho^J+\eta)\left(\|\mathbf{x}_0^\circ-\mathbf{x}_0\|^2 + 2R\sum_{i\in\mathcal{I}}\|\mathbf{x}_i^\circ-\mathbf{x}_{i+1}^\circ\|\right) + L_1 + \frac{\gamma^2}{2}\|T_I\mathbf{g}(\mathbf{x}_I)\|^2 + \gamma^2G^2\sum_{i\in\mathcal{I}}(T_i-T_{i+1})^2\\
&\overset{(b)}{\leq} \frac{D^2 T_{\max}}{4\alpha}T + (\alpha\rho^J+\eta)\left(R^2+2R\Pi_{\mathbf{x}^\circ}\right) + \gamma^2G^2(T_{\max}^2+\Pi_T) \qquad (34)
\end{aligned}$$

where (a) follows by noting that Ψ_i, Δ_{i+1}, and Φ_i are telescoping terms, such that their sums over $i \in \mathcal{I}$ are upper bounded by $\|\mathbf{x}_0^\circ - \mathbf{x}_0\|^2$, L_1, and $\|T_I\mathbf{g}(\mathbf{x}_I)\|^2$, respectively; (b) follows from $\mathcal{X}_0$ being bounded in (16), $L_1 = \frac{1}{2}\|\mathbf{Q}_1\|^2 = \frac{1}{2}\|\gamma\mathbf{g}(\mathbf{x}_0)T_0\|^2 \leq \frac{1}{2}\gamma^2G^2T_{\max}^2$, $\|T_I\mathbf{g}(\mathbf{x}_I)\|^2 \leq G^2T_{\max}^2$, and the definitions of $\Pi_{\mathbf{x}^\circ}$ in (17) and Π_T in (18). ■

The dynamic regret bound (25) in Theorem 1 improves as J increases. When J is large enough, we provide another dynamic regret bound for PQGA below.

Theorem 2. For J satisfying $2\rho^{J+1} < 1$, if we choose $\alpha \geq T_{\max}L$, $\eta \geq \max\{4\alpha, \beta^2\gamma^2T_{\max}^2\}$, and $\gamma > 0$, the dynamic regret of PQGA is upper bounded for any $\xi > 0$ by

$$\mathrm{RE_d}(T) \leq \frac{1}{4\xi}\Pi_\nabla + \frac{L+\xi}{1-2\rho^{J+1}}\left(R^2 + \frac{1}{\alpha+\varrho}[\gamma^2G^2(T_{\max}^2+\Pi_T) + \eta R(R+2\Pi_{\mathbf{x}^\circ})]\right) \qquad (35)$$

where $\Pi_\nabla \triangleq \sum_{i\in\mathcal{I}}\|\frac{T_i}{S_i}\sum_{s\in\mathcal{S}_i}\nabla f_{\tau_i^s}(\mathbf{x}_i^\circ)\|^2$ is the accumulated squared gradients.

Proof: We have

$$\begin{aligned}
\mathrm{RE_d}(T) = \sum_{i\in\mathcal{I}}\frac{T_i}{S_i}\sum_{s\in\mathcal{S}_i}\left(f_{\tau_i^s}(\mathbf{x}_i)-f_{\tau_i^s}(\mathbf{x}_i^\circ)\right) &\overset{(a)}{\leq} \sum_{i\in\mathcal{I}}\frac{T_i}{S_i}\sum_{s\in\mathcal{S}_i}[\nabla f_{\tau_i^s}(\mathbf{x}_i^\circ)]^T(\mathbf{x}_i-\mathbf{x}_i^\circ) + L\|\mathbf{x}_i-\mathbf{x}_i^\circ\|^2\\
&\overset{(b)}{\leq} \frac{1}{4\xi}\Pi_\nabla + (L+\xi)\sum_{i\in\mathcal{I}}\|\mathbf{x}_i-\mathbf{x}_i^\circ\|^2 \qquad (36)
\end{aligned}$$

where (a) follows from $f_t(\mathbf{x})$ being $2L$-smooth in (11), and (b) is because $\mathbf{a}^T\mathbf{b} \leq \frac{1}{4\xi}\|\mathbf{a}\|^2 + \xi\|\mathbf{b}\|^2$ for any $\xi > 0$ and Π_∇ being defined under (35).

We now bound $\sum_{i\in\mathcal{I}}\|\mathbf{x}_i - \mathbf{x}_i^\circ\|^2$ on the RHS of (36). From the inequality $\|\mathbf{a}+\mathbf{b}\|^2 \leq$

$2(\|\mathbf{a}\|^2+\|\mathbf{b}\|^2)$ and the bound on $\mathcal{X}_0$ in (16), we have

$$\sum_{i\in\mathcal{I}}\|\mathbf{x}_i-\mathbf{x}_i^\circ\|^2=\|\mathbf{x}_0-\mathbf{x}_0^\circ\|^2+\sum_{i\in\mathcal{I}}\|\mathbf{x}_{i+1}-\mathbf{x}_{i+1}^\circ\|^2\le R^2+2\sum_{i\in\mathcal{I}}\left(\|\mathbf{x}_{i+1}-\mathbf{x}_i^\circ\|^2+\|\mathbf{x}_i^\circ-\mathbf{x}_{i+1}^\circ\|^2\right). \tag{37}$$

We then bound $\sum_{i\in\mathcal{I}}\|\mathbf{x}_{i+1}-\mathbf{x}_i^\circ\|^2$ on the RHS of (37). From $f_{\tau_i^s}(\mathbf{x})$ being $2L$-smooth over $\mathcal{X}_0$ in (11), we have

$$f_{\tau_i^s}(\mathbf{x}_{i+1})\le f_{\tau_i^s}(\tilde{\mathbf{x}}_i^J)+[\nabla f_{\tau_i^s}(\tilde{\mathbf{x}}_i^J)]^T(\mathbf{x}_{i+1}-\tilde{\mathbf{x}}_i^J)+L\|\mathbf{x}_{i+1}-\tilde{\mathbf{x}}_i^J\|^2,\quad\forall s\in\mathcal{S}_i. \tag{38}$$

From $f_{\tau_i^s}(\mathbf{x})$ being 2ϱ-strongly convex over $\mathcal{X}_0$ in (10), we have

$$f_{\tau_i^s}(\mathbf{x}_i^\circ)\ge f_{\tau_i^s}(\tilde{\mathbf{x}}_i^J)+[\nabla f_{\tau_i^s}(\tilde{\mathbf{x}}_i^J)]^T(\mathbf{x}_i^\circ-\tilde{\mathbf{x}}_i^J)+\varrho\|\mathbf{x}_i^\circ-\tilde{\mathbf{x}}_i^J\|^2,\quad\forall s\in\mathcal{S}_i. \tag{39}$$

We can show that (26) in the proof of Theorem 1 still holds. Applying (38) and (39) to the LHS and RHS of (26), respectively, and rearranging terms, we have

$$\begin{aligned}\alpha\|\mathbf{x}_{i+1}-\mathbf{x}_i^\circ\|^2\le{}&\frac{T_i}{S_i}\sum_{s\in\mathcal{S}_i}\left(f_{\tau_i^s}(\mathbf{x}_i^\circ)-f_{\tau_i^s}(\mathbf{x}_{i+1})\right)-[\mathbf{Q}_{i+1}+\gamma T_i\mathbf{g}(\mathbf{x}_i)]^T[\gamma T_{i+1}\mathbf{g}(\mathbf{x}_{i+1})]-\eta\|\mathbf{x}_{i+1}-\mathbf{x}_i\|^2\\&+\eta(\|\mathbf{x}_i-\mathbf{x}_i^\circ\|^2-\|\mathbf{x}_{i+1}-\mathbf{x}_i^\circ\|^2)+(\alpha-T_i\varrho)\|\tilde{\mathbf{x}}_i^J-\mathbf{x}_i^\circ\|^2-(\alpha-T_iL)\|\mathbf{x}_{i+1}-\tilde{\mathbf{x}}_i^J\|^2.\end{aligned} \tag{40}$$

We now bound the right-hand side of (40). Noting that $\frac{T_i}{S_i}\sum_{s\in\mathcal{S}_i}f_{\tau_i^s}(\mathbf{x})$ is $2T_i\varrho$-strongly convex over $\mathcal{X}_0$, from the definition of $\mathbf{x}_i^\circ$ in (5), and applying Lemma 3 again, we have

$$\frac{T_i}{S_i}\sum_{s\in\mathcal{S}_i}f_{\tau_i^s}(\mathbf{x}_i^\circ)\le\frac{T_i}{S_i}\sum_{s\in\mathcal{S}_i}f_{\tau_i^s}(\mathbf{x}_{i+1})-T_i\varrho\|\mathbf{x}_{i+1}-\mathbf{x}_i^\circ\|^2. \tag{41}$$

We can show that (28) and (32) in the proof of Theorem 1 still hold. Substituting (28), (32), and (41) into the RHS of (40) and rearranging terms, we have

$$\begin{aligned}&(\alpha+T_i\varrho)\|\mathbf{x}_{i+1}-\mathbf{x}_i^\circ\|^2\\&\le-(\alpha-T_iL)\|\mathbf{x}_{i+1}-\tilde{\mathbf{x}}_i^J\|^2-(\eta-\beta^2\gamma^2T_i^2)\|\mathbf{x}_i-\mathbf{x}_{i+1}\|^2+(\alpha-T_i\varrho)\|\tilde{\mathbf{x}}_i^J-\mathbf{x}_i^\circ\|^2\\&\quad-\eta\|\mathbf{x}_i^\circ-\mathbf{x}_{i+1}^\circ\|^2-\Delta_{i+1}+\frac{\gamma^2}{2}\Phi_i+\gamma^2G^2(T_i-T_{i+1})^2+\eta\Psi_i+2R\eta\|\mathbf{x}_i^\circ-\mathbf{x}_{i+1}^\circ\|\\&\overset{(a)}{\le}(\alpha-T_i\varrho)\rho^J\|\mathbf{x}_i-\mathbf{x}_i^\circ\|^2-\eta\|\mathbf{x}_i^\circ-\mathbf{x}_{i+1}^\circ\|^2-\Delta_{i+1}+\frac{\gamma^2}{2}\Phi_i+\gamma^2G^2(T_i-T_{i+1})^2+\eta\Psi_i+2R\eta\|\mathbf{x}_i^\circ-\mathbf{x}_{i+1}^\circ\|\end{aligned} \tag{42}$$

where (a) follows from $\alpha\ge T_{\max}L$ and $\eta\ge\beta^2\gamma^2T_{\max}^2$, and (27) in the proof of Theorem 1.

Dividing both sides of (42) by $\alpha+T_i\varrho$ and substituting it into (37), we have

$$\begin{aligned}\sum_{i\in\mathcal{I}}\|\mathbf{x}_i-\mathbf{x}_i^\circ\|^2\le{}&R^2-\sum_{i\in\mathcal{I}}\left(\frac{\eta}{\alpha+T_i\varrho}-2\right)\|\mathbf{x}_i^\circ-\mathbf{x}_{i+1}^\circ\|^2+2\sum_{i\in\mathcal{I}}\rho^{J+1}\|\mathbf{x}_i-\mathbf{x}_i^\circ\|^2\\&+\sum_{i\in\mathcal{I}}\frac{1}{\alpha+T_i\varrho}\left(-\Delta_{i+1}+\frac{\gamma^2}{2}\Phi_i+\gamma^2G^2(T_i-T_{i+1})^2+\eta\Psi_i+2R\eta\|\mathbf{x}_i^\circ-\mathbf{x}_{i+1}^\circ\|\right)\end{aligned}$$

$$\overset{(a)}{\leq} R^2 + 2\rho^{J+1}\sum_{i\in\mathcal{I}}\|\mathbf{x}_i - \mathbf{x}_i^\circ\|^2 + \frac{1}{\alpha+\varrho}\left[\gamma^2 G^2(T_{\max}^2 + \Pi_T) + \eta R(R + 2\Pi_{\mathbf{x}^\circ})\right] \tag{43}$$

where (a) follows from $\rho = \frac{\alpha-\varrho}{\alpha+\varrho}$, $\eta \geq 4\alpha \geq 2(\alpha + T_{\max}\varrho)$, and (b) in the proof of (34) for Theorem 1.

Substituting (43) into (36), on the condition that $2\rho^{J+1} < 1$, we have (35). ■

2) Bounding the Static Regret: Next, using the proof techniques for the dynamic regret $\text{RE}_\text{d}(T)$ in Theorem 1, we provide an upper bound on the static regret $\text{RE}_\text{s}(T)$ yielded by PQGA, given in the following theorem.

Theorem 3. For any $J \geq 0$, if we choose $\alpha \geq T_{\max}L$, $\eta \geq \beta^2\gamma^2 T_{\max}^2$, and $\gamma > 0$, the static regret of PQGA is upper bounded by

$$\text{RE}_\text{s}(T) \leq \frac{D^2 T_{\max}}{4\alpha}T + (\alpha\rho^J + \eta)R^2 + \gamma^2 G^2(T_{\max}^2 + \Pi_T). \tag{44}$$

Proof: (Proof outline) Replacing all the per-period optimizers $\{\mathbf{x}_i^\circ\}$ with the static offline benchmark $\mathbf{x}^\star$ in the proof of Theorem 1, we can show that for any $\alpha \geq T_{\max}L$, $\eta \geq \beta^2\gamma^2 T_{\max}$, and $\gamma > 0$, (33) still holds by redefining $\Psi_i \triangleq \|\mathbf{x}^\star - \mathbf{x}_i\|^2 - \|\mathbf{x}^\star - \mathbf{x}_{i+1}\|^2$ and $\psi_i = 0$. Summing the new version of (33) over $i \in \mathcal{I}$, and noting that Ψ_i is still telescoping, we complete the proof. ■

3) Bounding the Constraint Violation: We now proceed to provide an upper bound on the constraint violation $\text{VO}^c(T)$ for PQGA. We first relate the virtual queue vector $\mathbf{Q}_I$ to $\text{VO}^c(T)$ in the following lemma.

Lemma 5. The periodic virtual queue vector yielded by PQGA satisfies the following inequality:

$$\text{VO}^c(T) \leq \frac{1}{\gamma}\|\mathbf{Q}_I\|, \quad \forall c \in \mathcal{C}. \tag{45}$$

Proof: From the periodic virtual queue dynamics in (8), for any $c \in \mathcal{C}$ and $i \in \mathcal{I}$, we have

$$\gamma T_i g^c(\mathbf{x}_i) \leq Q_{i+1}^c - Q_i^c. \tag{46}$$

Summing (46) over $i \in \mathcal{I}$, we have

$$\text{VO}^c(T) = \sum_{i\in\mathcal{I}} T_i g^c(\mathbf{x}_i) \leq \frac{1}{\gamma}\sum_{i\in\mathcal{I}}(Q_{i+1}^c - Q_i^c) = \frac{1}{\gamma}(Q_I^c - Q_0^c) \overset{(a)}{=} \frac{1}{\gamma}Q_I^c \overset{(b)}{\leq} \frac{1}{\gamma}\|\mathbf{Q}_I\| \tag{47}$$

where (a) follows from $Q_0^c = 0$ by initialization, and (b) is because $\|\mathbf{a}\|_\infty \leq \|\mathbf{a}\|$. ■

Using Lemma 5, we can bound the constraint violation $\text{VO}^c(T)$ through an upper bound on the virtual queue vector $\mathbf{Q}_I$. The result is stated in the following theorem.

Theorem 4. For any $J \geq 0$, if we choose $\alpha, \eta, \gamma > 0$, the constraint violation of PQGA is upper bounded for any constraint $c \in \mathcal{C}$ by

$$\text{VO}^c(T) \leq 2GT_{\max} + \frac{(\alpha+\eta)R^2 + DRT_{\max}^2 + 2\gamma^2 G^2 T_{\max}}{\epsilon\gamma^2}. \tag{48}$$

Proof: Since $\mathbf{x}_{i+1}$ is chosen to solve **P2′**, for any $i \in \mathcal{I}$, we have

$$\begin{aligned}
&\frac{T_i}{S_i}\sum_{s\in\mathcal{S}_i}[\nabla f_{\tau_i^s}(\tilde{\mathbf{x}}_i^J)]^T(\mathbf{x}_{i+1}-\tilde{\mathbf{x}}_i^J) + \alpha\|\mathbf{x}_{i+1}-\tilde{\mathbf{x}}_i^J\|^2 + [\mathbf{Q}_{i+1}+\gamma T_i\mathbf{g}(\mathbf{x}_i)]^T[\gamma T_{i+1}\mathbf{g}(\mathbf{x}_{i+1})] + \eta\|\mathbf{x}_{i+1}-\mathbf{x}_i\|^2 \\
&\quad\leq \frac{T_i}{S_i}\sum_{s\in\mathcal{S}_i}[\nabla f_{\tau_i^s}(\tilde{\mathbf{x}}_i^J)]^T(\mathbf{x}'-\tilde{\mathbf{x}}_i^J) + \alpha\|\mathbf{x}'-\tilde{\mathbf{x}}_i^J\|^2 + [\mathbf{Q}_{i+1}+\gamma T_i\mathbf{g}(\mathbf{x}_i)]^T[\gamma T_{i+1}\mathbf{g}(\mathbf{x}')] + \eta\|\mathbf{x}'-\mathbf{x}_i\|^2. \quad (49)
\end{aligned}$$

Note that

$$\begin{aligned}
[\mathbf{Q}_{i+1}+\gamma T_i\mathbf{g}(\mathbf{x}_i)]^T[\gamma T_{i+1}\mathbf{g}(\mathbf{x}')] &\overset{(a)}{\leq} -\epsilon\gamma T_{i+1}[\mathbf{Q}_{i+1}+\gamma T_i\mathbf{g}(\mathbf{x}_i)]^T\mathbf{1} \overset{(b)}{\leq} -\epsilon\gamma T_{i+1}\|\mathbf{Q}_{i+1}+\gamma T_i\mathbf{g}(\mathbf{x}_i)\| \\
&\overset{(c)}{\leq} -\epsilon\gamma T_{i+1}(\|\mathbf{Q}_{i+1}\| - \|\gamma T_i\mathbf{g}(\mathbf{x}_i)\|) \qquad (50)
\end{aligned}$$

where (a) follows from $\mathbf{x}'$ being an interior point of $\mathbf{g}(\mathbf{x})$ in (15) and $\mathbf{Q}_{i+1}+\gamma T_i\mathbf{g}(\mathbf{x}_i) \succeq \mathbf{0}$ in (20), (b) is because $\|\mathbf{a}\| \leq \|\mathbf{a}\|_1$, and (c) follows from $|(\|\mathbf{a}\| - \|\mathbf{b}\|)| \leq \|\mathbf{a}-\mathbf{b}\|$ and $\|\mathbf{Q}_{i+1}\| \geq \|\gamma T_i\mathbf{g}(\mathbf{x}_i)\|$ in (21).

Substituting (50) into (49), and rearranging terms, we have

$$\begin{aligned}
\mathbf{Q}_{i+1}^T[\gamma T_{i+1}\mathbf{g}(\mathbf{x}_{i+1})] &\leq -\epsilon\gamma T_{i+1}(\|\mathbf{Q}_{i+1}\| - \|\gamma T_i\mathbf{g}(\mathbf{x}_i)\|) + \alpha\|\mathbf{x}'-\tilde{\mathbf{x}}_i^J\|^2 + \eta\|\mathbf{x}'-\mathbf{x}_i\|^2 \\
&\quad + \frac{T_i}{S_i}\sum_{s\in\mathcal{S}_i}[\nabla f_{\tau_i^s}(\tilde{\mathbf{x}}_i^J)]^T(\mathbf{x}'-\mathbf{x}_{i+1}) - [\gamma T_i\mathbf{g}(\mathbf{x}_i)]^T[\gamma T_{i+1}\mathbf{g}(\mathbf{x}_{i+1})] \\
&\overset{(a)}{\leq} -\epsilon\gamma T_{i+1}\|\mathbf{Q}_{i+1}\| + \epsilon\gamma^2 T_{i+1}\|T_i\mathbf{g}(\mathbf{x}_i)\| + \alpha\|\mathbf{x}'-\tilde{\mathbf{x}}_i^J\|^2 + \eta\|\mathbf{x}'-\mathbf{x}_i\|^2 \\
&\quad + \frac{T_i}{S_i}\sum_{s\in\mathcal{S}_i}\|\nabla f_{\tau_i^s}(\tilde{\mathbf{x}}_i^J)\|\|\mathbf{x}'-\mathbf{x}_{i+1}\| + \gamma^2\|T_i\mathbf{g}(\mathbf{x}_i)\|\|T_{i+1}\mathbf{g}(\mathbf{x}_{i+1})\| \\
&\overset{(b)}{\leq} -\epsilon\gamma T_{i+1}\|\mathbf{Q}_{i+1}\| + \epsilon\gamma^2 GT_{i+1}T_i + (\alpha+\eta)R^2 + DRT_i + \gamma^2G^2T_{i+1}T_i \qquad (51)
\end{aligned}$$

where (a) is because $|\mathbf{a}^T\mathbf{b}| \leq \|\mathbf{a}\|\|\mathbf{b}\|$; and (b) follows from the bound on $\mathbf{g}(\mathbf{x})$ in (14), the bound on $\mathcal{X}_0$ in (16), and the bound on $\nabla f_t(\mathbf{x})$ in (12). From (23) in Lemma 2, we have

$$\Delta_{i+1} \leq \mathbf{Q}_{i+1}^T[\gamma T_{i+1}\mathbf{g}(\mathbf{x}_{i+1})] + \|\gamma T_{i+1}\mathbf{g}(\mathbf{x}_{i+1})\|^2 \leq \mathbf{Q}_{i+1}^T[\gamma T_{i+1}\mathbf{g}(\mathbf{x}_{i+1})] + \gamma^2G^2T_{i+1}^2. \tag{52}$$

Substituting (51) into (52), we have

$$\Delta_{i+1} \leq -\epsilon\gamma T_{i+1}\|\mathbf{Q}_{i+1}\| + \epsilon\gamma^2 G T_{i+1}T_i + (\alpha+\eta)R^2 + DRT_i + \gamma^2 G^2 T_{i+1}T_i + \gamma^2 G^2 T_{i+1}^2. \tag{53}$$

Noting that $1 \leq T_i \leq T_{\max}$ for any $i \in \mathcal{I}$, from (53), the sufficient condition for $\Delta_{i+1} < 0$ is

$$\|\mathbf{Q}_{i+1}\| > \gamma G T_{\max} + \frac{(\alpha+\eta)R^2 + DRT_{\max}^2 + 2\gamma^2 G^2 T_{\max}}{\epsilon\gamma}.$$

If the above inequality holds, we have $\|\mathbf{Q}_{i+2}\| \leq \|\mathbf{Q}_{i+1}\|$, *i.e.,* the virtual queue length decreases; otherwise, from the virtual queue bound in (22), there is a maximum increase from $\|\mathbf{Q}_{i+1}\|$ to $\|\mathbf{Q}_{i+2}\|$ since $\|\mathbf{Q}_{i+2}\| \leq \|\mathbf{Q}_{i+1}\| + \|\gamma \mathbf{g}(\mathbf{x}_{i+1})T_{i+1}\| \leq \|\mathbf{Q}_{i+1}\| + \gamma G T_{\max}$. Therefore, the virtual queue vector $\mathbf{Q}_I$ is upper bounded by

$$\|\mathbf{Q}_I\| \leq 2\gamma G T_{\max} + \frac{(\alpha+\eta)R^2 + DRT_{\max}^2 + 2\gamma^2 G^2 T_{\max}}{\epsilon\gamma}.$$

Substituting the above inequality into (45) in Lemma 5, we have (48). ■

C. Discussion on the Performance Bounds

In this section, we discuss the regret and constraint violation bounds of PQGA. To describe the level of time variation of the dynamic benchmark and update periods, we define parameters $\nu \geq 0$ and $\delta \geq 0$ such that

$$\Pi_{\mathbf{x}^\circ} = \mathcal{O}(T^\nu), \tag{54}$$

$$\Pi_T = \mathcal{O}(T^\delta). \tag{55}$$

We show below that suitable values of parameters α, η, and γ for PQGA depend on whether ν and δ are known. Furthermore, the regret and constraint violation bounds also depend on the number of aggregated gradient descent steps J. We summarize the performance bounds of PQGA in Tables II and III.

1) Regret and Constraint Violation Bounds for General J: From Theorems 1, 3, and 4, we can derive the following two corollaries regarding the regret and constraint violation bounds for any $J \geq 0$. The results can be easily obtained by substituting the chosen parameters α, η, and γ into the general performance bounds in (25), (44), and (48), and we omit the algebraic details to avoid redundancy.

Corollary 1. (Algorithm parameters with knowledge of ν and δ) Let $\gamma^2 = T^\kappa$, where $\kappa \in [0, \frac{1}{2}]$ is some trade-off parameter that can be freely chosen and $\eta = \beta^2\gamma^2 T_{\max}^2$. Then, for

TABLE II
DYNAMIC REGRET, STATIC REGRET, AND CONSTRAINT VIOLATION BOUNDS OF PQGA FOR ANY J ($\Pi_{\mathbf{x}^\circ} = \mathcal{O}(T^\nu)$ AND $\Pi_T = \mathcal{O}(T^\delta)$)

$\Pi_T = \mathcal{O}(1)$	Know ν and δ	$\text{RE}_\text{d}(T)$	$\text{RE}_\text{s}(T)$	$\text{VO}^c(T)$
No	Yes	$\mathcal{O}(\max\{T^{\frac{1+\nu}{2}}, T^{\delta+\kappa}\})$	$\mathcal{O}(\max\{T^{\frac{1}{2}}, T^{\delta+\kappa}\})$	$\mathcal{O}(T^{\frac{1}{2}-\kappa})$
No	No	$\mathcal{O}(\max\{T^{\frac{1}{2}+\nu}, T^{\delta}\})$	$\mathcal{O}(\max\{T^{\frac{1}{2}}, T^{\delta}\})$	$\mathcal{O}(T^{\frac{1}{2}})$
Yes	Yes	$\mathcal{O}(T^{\frac{1+\nu}{2}})$	$\mathcal{O}(T^{\frac{1}{2}})$	$\mathcal{O}(1)$
Yes	No	$\mathcal{O}(T^{\frac{1}{2}+\nu})$	$\mathcal{O}(T^{\frac{1}{2}})$	$\mathcal{O}(1)$

TABLE III
IMPROVED DYNAMIC REGRET AND CONSTRAINT VIOLATION BOUNDS OF PQGA FOR A LARGE J ($\Pi_{\mathbf{x}^\circ} = \mathcal{O}(T^\nu)$ AND $\Pi_T = \mathcal{O}(T^\delta)$)

$\Pi_T = \mathcal{O}(1)$	Know ν and δ	$\text{RE}_\text{d}(T)$	$\text{VO}^c(T)$
No	No	$\mathcal{O}(\max\{T^{\nu}, T^{\delta}\})$	$\mathcal{O}(1)$
Yes	No	$\mathcal{O}(T^{\nu})$	$\mathcal{O}(1)$

any $J \geq 0$, $\text{RE}_\text{d}(T) = \mathcal{O}(\max\{T^{\frac{1+\nu}{2}}, T^{\delta+\kappa}\})$ if we choose $\alpha = T_{\max} L T^{\frac{1-\nu}{2}}$, and $\text{RE}_\text{s}(T) = \mathcal{O}(\max\{T^{\frac{1}{2}}, T^{\delta+\kappa}\})$ if we choose $\alpha = T_{\max} L T^{\frac{1}{2}}$. In both cases, $\text{VO}^c(T) = \mathcal{O}(T^{\frac{1}{2}-\kappa})$. Therefore, for any $0 \leq \nu < 1$ and $0 \leq \delta < 1$, and any κ such that $\kappa + \delta < 1$, both the dynamic and static regrets are sublinear and the constraint violation are sublinear.

Corollary 2. (Algorithm parameters without knowledge of ν or δ) Let $\alpha = T_{\max} L T^{\frac{1}{2}}$, $\eta = \beta^2 \gamma^2 T_{\max}^2$, and $\gamma^2 = 1$ in PQGA. Then, for any $J \geq 0$, $\text{RE}_\text{d}(T) = \mathcal{O}(\max\{T^{\frac{1}{2}+\nu}, T^{\delta}\})$, $\text{RE}_\text{s}(T) = \mathcal{O}(\max\{T^{\frac{1}{2}}, T^{\delta}\})$, and $\text{VO}^c(T) = \mathcal{O}(T^{\frac{1}{2}})$.

From Corollaries 1 and 2, a sufficient condition for PQGA to yield sublinear regrets under periodic updates is that the system variation measures $\Pi_{\mathbf{x}^\circ}$ and Π_T grow sublinearly over time. In many online applications, the system tends to stabilize over time, leading to sublinear system variation and thus sublinear regrets.

Remark 5. Sublinearly of the system variation measures is necessary to have sublinear dynamic regret for OCO [10]. Otherwise, if the system varies too fast over time, no online algorithm can track it due to the lack of in-time information. This can be seen from the dynamic regret bounds derived in [7], [13]-[17], [21], [24], [25] even under the standard per-time-slot update setting.

Remark 6. With unknown time horizon T, the standard doubling trick [3], [14], [22] can be applied to extend PQGA into one that has similar regret bounds.

2) Improved Dynamic Regret Bound for Large J: From Theorems 2 and 4, we can derive the following corollaries regarding the dynamic regret and constraint violation bounds for PQGA, when the number of aggregated gradient descent steps J is large enough.

Corollary 3. Suppose $\Pi_\nabla = \mathcal{O}(T^\nu)$.[3] Let $\alpha = T_{\max}L$, $\eta = \max\{4\alpha, \beta^2\gamma^2 T_{\max}^2\}$, and $\gamma = 1$. Then, for any $J \geq 0$ such that $2\rho^{J+1} < 1$, $\text{RE}_\text{d}(T) = \mathcal{O}(\max\{T^\nu, T^\delta\})$ and $\text{VO}^c(T) = \mathcal{O}(1)$. Therefore, for any $0 \leq \nu < 1$ and $0 \leq \delta < 1$, both the dynamic regret and the constraint violation are sublinear.

Remark 7. When J is large enough, the optimal algorithm parameters of PQGA do not require the knowledge of the system variation measures, *i.e.,* ν and δ, or the total time horizon T.

3) A Special Case of Bounded Π_T: The following corollaries provide the regret and constraint violation bounds when the accumulated variation of update periods is upper bounded by a constant, *i.e.,* $\Pi_T = \mathcal{O}(1)$. In particular, this includes the case where the update periods are fixed over time. The results are obtained by setting $\delta = 0$ in Corollaries 1-3, respectively.

Corollary 4. (Algorithm parameters with knowledge of ν and δ) Let $\gamma^2 = T^{\frac{1}{2}}$ and $\eta = \beta^2\gamma^2 T_{\max}^2$. Then, for any $J \geq 0$, $\text{RE}_\text{d}(T) = \mathcal{O}(T^{\frac{1+\nu}{2}})$ if we chose $\alpha = T_{\max}LT^{\frac{1-\nu}{2}}$, and $\text{RE}_\text{s}(T) = \mathcal{O}(T^{\frac{1}{2}})$ if we choose $\alpha = T_{\max}LT^{\frac{1}{2}}$. In both cases, $\text{VO}^c(T) = \mathcal{O}(1)$.

Corollary 5. (Algorithm parameters without knowledge of ν or δ) Let $\alpha = T_{\max}LT^{\frac{1}{2}}$, $\eta = \beta^2\gamma^2 T_{\max}^2$, and $\gamma^2 = T^{\frac{1}{2}}$ in PQGA. Then, for any $J \geq 0$, $\text{RE}_\text{d}(T) = \mathcal{O}(T^{\frac{1}{2}+\nu})$, $\text{RE}_\text{s}(T) = \mathcal{O}(T^{\frac{1}{2}})$, and $\text{VO}^c(T) = \mathcal{O}(1)$.

Corollary 6. Suppose $\Pi_\nabla = \mathcal{O}(T^\nu)$. Let $\alpha = T_{\max}L$, $\eta = \max\{4\alpha, \beta^2\gamma^2 T_{\max}^2\}$, and $\gamma = 1$. Then, for any $J \geq 0$ such that $2\rho^{J+1} < 1$, $\text{RE}_\text{d}(T) = \mathcal{O}(T^\nu)$ and $\text{VO}^c(T) = \mathcal{O}(1)$.

Remark 8. PQGA can be applied to the special case of per-time-slot updates [18]-[25]. Its regret and constraint violation bounds are given by Corollaries 4 and 5, with $T_{\max} = 1$. In this case, PQGA recovers the known best $\mathcal{O}(T^{\frac{1}{2}})$ static regret and $\mathcal{O}(1)$ constraint violation in [22]. Furthermore, while [22] does not provide a dynamic regret bound, here we show that PQGA

[3]The accumulated squared gradients Π_∇ can be very small [16]. In particular, we have $\Pi_\nabla = 0$ if $\mathbf{x}_i^\circ$ is an interior point of $\mathcal{X}_0$ (or there is no short-term constraint), *i.e.,* $\sum_{s\in\mathcal{S}_i} \nabla f_{\tau_i^s}(\mathbf{x}_i^\circ) = \mathbf{0}$ for any $i \in \mathcal{I}$.

achieves $\mathcal{O}(T^{\frac{1+\nu}{2}})$ dynamic regret.[4]

Remark 9. By increasing J, the dynamic regret of PQGA improves from $\mathcal{O}(T^{\frac{1+\nu}{2}})$ in Corollary 4 to $\mathcal{O}(T^{\nu})$ in Corollary 6, while maintaining the $\mathcal{O}(1)$ constraint violation. To the best of our knowledge, even under the standard per-time-slot update setting, no known constrained OCO algorithm has simultaneously achieved $\mathcal{O}(T^{\nu})$ dynamic regret and $\mathcal{O}(1)$ constraint violation.

V. Application to Massive MIMO System with Multiple Service Providers

In many wireless systems, CSI is only available after a series of channel estimation, quantization, and feedback processes. This challenge is especially acute with massive MIMO systems, where the channel state space is large and the channel state can fluctuate quickly over time. Online learning provides the tools to solve a variety of problems in dynamic MIMO systems.

As an example to study the performance of PQGA in practical systems, we apply it to online network virtualization with massive MIMO antennas, where multiple service providers (SPs) simultaneously share all the antennas and channel resources provided by an infrastructure provider (InP). Most of the existing works on MIMO virtualization have focused on offline problems [32]-[37]. Furthermore, these works enforce strict physical isolation among the SPs, which suffer from performance loss in comparison with the spatial isolation approach in [30] and [38]. The virtualization solutions in [30] and [38] are online but they are based on Lyapunov optimization and require the current CSI. Furthermore, neither of them considers periodic precoder updates, which are essential to practical LTE and 5G NR networks.

A. Online Precoding-Based Massive MIMO Network Virtualization

We consider an InP performing network virtualization in a massive MIMO cellular network. In each cell, the InP owns a base station (BS) equipped with N antennas, serving M SPs. Let $\mathcal{M} = \{1, \ldots, M\}$. Each SP m has K_m users. Let the total number of users in the cell be K. We consider a time-slotted system with time indexed by t. Let $\mathbf{H}_t^m \in \mathbb{C}^{K_m \times N}$ be the local CSI between the BS and the K_m users of SP m at time t.

[4]The analysis in [22] is for convex loss functions. We can show that PQGA still yields $\mathcal{O}(T^{\frac{1+\nu}{2}})$ dynamic regret, $\mathcal{O}(T^{\frac{1}{2}})$ static regret, and $\mathcal{O}(1)$ constraint violation for convex loss functions with some care of technical details and hence is omitted.

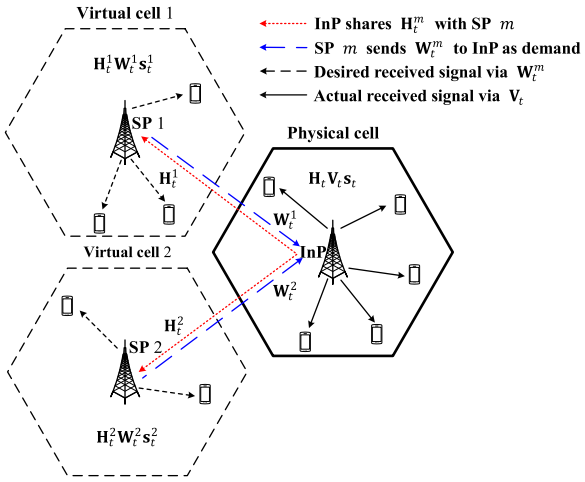


Fig. 2. An illustration of idealized massive MIMO virtualization in a cell with one InP and two SPs serving users in their respective virtual cell.

1) Precoding-Based Network Virtualization: For ease of exposition, we first consider an idealized massive MIMO virtualization framework, where CSI is fedback per time slot without delay, as shown in Fig. 2. At each time slot t, the InP shares the corresponding local CSI $\mathbf{H}_t^m$ with SP m, and it allocates transmit power P_m to the SP. The power allocation is limited by the total transmit power budget $P_{\max}$, *i.e.,* $\sum_{m\in\mathcal{M}} P_m \leq P_{\max}$. Using $\mathbf{H}_t^m$, each SP m designs its own precoding matrix $\mathbf{W}_t^m \in \mathbb{C}^{N\times K_m}$ based on the service needs of its users, while ensuring $\|\mathbf{W}_t^m\|_F^2 \leq P_m$. The SP then sends $\mathbf{W}_t^m$ to the InP as its service demand. Note that each SP m designs $\mathbf{W}_t^m$ based only on its local CSI, not needing to be aware of the users of the other SPs. For SP m, its *desired* received signal vector $\tilde{\mathbf{y}}_t^m$ at its K_m users is given by

$$\tilde{\mathbf{y}}_t^m = \mathbf{H}_t^m\mathbf{W}_t^m\mathbf{s}_t^m, \quad \forall m \in \mathcal{M}$$

where $\mathbf{s}_t^m$ is the transmitted signal vector from SP m to its K_m users. Let $\tilde{\mathbf{y}}_t \triangleq [\tilde{\mathbf{y}}_t^{1H}, \ldots, \tilde{\mathbf{y}}_t^{MH}]^H$ be the desired received signal vector at all K users, $\mathbf{D}_t \triangleq \text{blkdiag}\{\mathbf{H}_t^1\mathbf{W}_t^1, \ldots, \mathbf{H}_t^M\mathbf{W}_t^M\}$ be the virtualization demand made by the SPs, and $\mathbf{s}_t \triangleq [\mathbf{s}_t^{1H}, \ldots, \mathbf{s}_t^{MH}]^H$. Then we have $\tilde{\mathbf{y}}_t = \mathbf{D}_t\mathbf{s}_t$. We assume that the transmitted signals to all K users are independent to each other, with $\mathbb{E}\{\mathbf{s}_t\mathbf{s}_t^H\} = \mathbf{I}, \forall t$.

At each time slot t, the InP has the global CSI $\mathbf{H}_t = [\mathbf{H}_t^{1H}, \ldots, \mathbf{H}_t^{MH}]^H \in \mathbb{C}^{K\times N}$ and designs the *actual* global downlink precoding matrix $\mathbf{V}_t \triangleq [\mathbf{V}_t^1, \ldots, \mathbf{V}_t^M] \in \mathbb{C}^{N\times K}$ to serve all K users, where $\mathbf{V}_t^m \in \mathbb{C}^{N\times K_m}$ is the actual downlink precoding matrix for SP m. Then, the actual received

signal vector $\mathbf{y}_t^m$ at the users of SP m is given by

$$\mathbf{y}_t^m = \mathbf{H}_t^m \mathbf{V}_t^m \mathbf{s}_t^m + \sum_{l \neq m, l \in \mathcal{M}} \mathbf{H}_t^m \mathbf{V}_t^l \mathbf{s}_t^l, \quad \forall m \in \mathcal{M}$$

where the second term is the inter-SP interference from the other SPs to the users of SP m. The actual received signal vector $\mathbf{y}_t \triangleq [\mathbf{y}_t^{1H}, \ldots, \mathbf{y}_t^{MH}]^H$ at all K users is given by $\mathbf{y}_t = \mathbf{H}_t \mathbf{V}_t \mathbf{s}_t$.

For downlink massive MIMO network virtualization, the InP designs the actual precoding matrix $\mathbf{V}_t$ to mitigate the inter-SP interference in order to meet the virtualization demand $\mathbf{D}_t$ received from the SPs. The expected deviation of the actual received signals from that of the SPs' virtualization demand is given by $\mathbb{E}\{\|\mathbf{y}_t - \tilde{\mathbf{y}}_t\|_F^2\} = \|\mathbf{H}_t \mathbf{V}_t - \mathbf{D}_t\|_F^2$. Therefore, we define the *precoding deviation* for any precoding matrix $\mathbf{V}$ as follows:

$$f_t(\mathbf{V}) \triangleq \|\mathbf{H}_t \mathbf{V} - \mathbf{D}_t\|_F^2, \quad \forall t \in \mathcal{T} \tag{56}$$

which we use as the design metric for massive MIMO network virtualization. Note that $f_t(\mathbf{V})$ naturally quantifies the difference between the actual global precoder executed at the BS and the virtual local precoders demanded by the SPs. Furthermore, it is strongly convex in $\mathbf{V}$.

2) Online Precoding Optimization with Periodic Updates: Under the transmission structure of a typical cellular network, such as LTE and 5G NR, we consider an online periodic virtualization demand-response mechanism. An update period may correspond to the duration of one or multiple resource blocks and can vary over time. Within each update period $i \in \mathcal{I}$, the InP, which is the decision maker as defined in Section III, receives multiple delayed CSI $\mathbf{H}_t$ and virtualization demand $\mathbf{D}_t$ feedbacks for $t \in \mathcal{T}_i$. At the beginning of each update period i, the InP determines $\mathbf{V}_i$ in the compact convex set

$$\mathcal{V}_0 \triangleq \{\mathbf{V} : \|\mathbf{V}\|_F^2 \leq P_{\max}\} \tag{57}$$

to meet the short-term transmit power constraint. We also consider a long-term transmit power constraint, with

$$g(\mathbf{V}) \triangleq \|\mathbf{V}\|_F^2 - \bar{P} \tag{58}$$

being the long-term transmit power constraint function, where $\bar{P} \leq P_{\max}$ is the average transmit power budget.

Then, our online optimization problem for MIMO network virtualization is in the same form

as **P1**, with the loss function, short-term constraint, and long-term constraint function given in (56), (57), and (58), respectively.

B. Online Precoding Solution

Using the proposed PQGA algorithm, at the beginning of each update period $i+1$, we first initialize an intermediate precoder $\tilde{\mathbf{V}}_i^0 = \mathbf{V}_i$. If $J > 0$, for each $j \in \mathcal{J}$, we solve the following precoder optimization problem for $\tilde{\mathbf{V}}_i^j$:

$$\min_{\mathbf{V}\in\mathcal{V}_0} \frac{T_i}{S_i}\sum_{s\in\mathcal{S}_i} 2\Re\{\mathrm{tr}\{[\nabla_{\tilde{\mathbf{V}}_i^{j-1*}} f_{\tau_i^s}(\tilde{\mathbf{V}}_i^{j-1})]^H(\mathbf{V}-\tilde{\mathbf{V}}_i^{j-1})\}\} + \alpha\|\mathbf{V}-\tilde{\mathbf{V}}_i^{j-1}\|_F^2$$

where $\nabla_{\tilde{\mathbf{V}}_i^{j-1*}} f_{\tau_i^s}(\tilde{\mathbf{V}}_i^{j-1}) = \mathbf{H}_{\tau_i^s}^H(\mathbf{H}_{\tau_i^s}\tilde{\mathbf{V}}_i^{j-1} - \mathbf{D}_{\tau_i^s})$. This is equivalent to performing projected aggregated gradient descent with a closed-form solution for $\tilde{\mathbf{V}}_i^j$, given by

$$\tilde{\mathbf{V}}_i^j = \begin{cases} \tilde{\mathbf{X}}_i^j, & \text{if } \|\tilde{\mathbf{X}}_i^j\|_F^2 \le P_{\max} \\ \sqrt{P_{\max}}\dfrac{\tilde{\mathbf{X}}_i^j}{\|\tilde{\mathbf{X}}_i^j\|_F}, & \text{o.w.} \end{cases} \tag{59}$$

where $\tilde{\mathbf{X}}_i^j = \tilde{\mathbf{V}}_i^{j-1} - \frac{T_i}{\alpha S_i}\sum_{s\in\mathcal{S}_i}\mathbf{H}_{\tau_i^s}^H(\mathbf{H}_{\tau_i^s}\tilde{\mathbf{V}}_i^{j-1} - \mathbf{D}_{\tau_i^s})$.

After performing J-step aggregated gradient descent, with both $\tilde{\mathbf{V}}^J$ and $\mathbf{V}_i$, we solve the following precoder optimization problem for the actual precoding matrix $\mathbf{V}_{i+1}$:

$$\begin{aligned}\mathbf{P3}'\!:\ \min_{\mathbf{V}\in\mathcal{V}_0}\ & \frac{T_i}{S_i}\sum_{s\in\mathcal{S}_i} 2\Re\{\mathrm{tr}\{[\nabla_{\tilde{\mathbf{V}}_i^{J*}} f_{\tau_i^s}(\tilde{\mathbf{V}}_i^J)]^H(\mathbf{V}-\tilde{\mathbf{V}}_i^J)\}\} + \alpha\|\mathbf{V}-\tilde{\mathbf{V}}_i^J\|_F^2 + \eta\|\mathbf{V}-\mathbf{V}_i\|_F^2 \\ & + [Q_{i+1} + \gamma T_i g(\mathbf{V}_i)][\gamma T_{i+1} g(\mathbf{V})]\end{aligned}$$

where Q_{i+1} is a periodic virtual queue with updating rule in (8). Since **P3′** is a strongly convex optimization problem with strong duality, we solve it by inspecting Karush-Kuhn-Tucker (KKT) conditions [39]. The Lagrangian for **P3′** is

$$\begin{aligned}L(\mathbf{V},\lambda) = & \frac{T_i}{S_i}\sum_{s\in\mathcal{S}_i} 2\Re\{\mathrm{tr}\{[\nabla_{\tilde{\mathbf{V}}_i^{J*}} f_{\tau_i^s}(\tilde{\mathbf{V}}_i^J)]^H(\mathbf{V}-\tilde{\mathbf{V}}_i^J)\}\} + \alpha\|\mathbf{V}-\tilde{\mathbf{V}}_i^J\|_F^2 + \eta\|\mathbf{V}-\mathbf{V}_i\|_F^2 \\ & + [Q_{i+1} + \gamma T_i g(\mathbf{V}_i)][\gamma T_{i+1} g(\mathbf{V})] + \lambda(\|\mathbf{V}\|_F^2 - P_{\max})\end{aligned}$$

where λ is the Lagrange multiplier associated with the short-term transmit power constraint in (57). The KKT conditions for $(\mathbf{V}^\star, \lambda^\star)$ being globally optimal are given by $\|\mathbf{V}^\star\|_F^2 - P_{\max} \le 0$,

$\lambda^\star \geq 0$, $\lambda^\star(\|\mathbf{V}^\star\|_F^2 - P_{\max}) = 0$, and

$$\mathbf{V}^\star = \frac{\alpha\tilde{\mathbf{V}}_i^J + \eta\mathbf{V}_i - \frac{T_i}{S_i}\sum_{s\in\mathcal{S}_i}\mathbf{H}_{\tau_i^s}^H(\mathbf{H}_{\tau_i^s}\tilde{\mathbf{V}}_i^J - \mathbf{D}_{\tau_i^s})}{\alpha + \eta + [Q_{i+1} + \gamma T_i g(\mathbf{V}_i)]\gamma T_{i+1} + \lambda^\star}, \tag{60}$$

which follows from setting $\nabla_{\mathbf{V}^*}L(\mathbf{V}, \lambda) = \mathbf{0}$. From the KKT conditions, and noting that $\lambda^\star$ serves as a power regularization factor for $\mathbf{V}^\star$ in (60), we have a closed-form solution for $\mathbf{V}_{i+1}$, given by

$$\mathbf{V}_{i+1} = \begin{cases} \mathbf{X}_i, & \text{if } \|\mathbf{X}_i\|_F^2 \leq P_{\max} \\ \sqrt{P_{\max}}\frac{\mathbf{X}_i}{\|\mathbf{X}_i\|_F}, & \text{o.w.} \end{cases} \tag{61}$$

where $\mathbf{X}_i = \frac{\alpha\tilde{\mathbf{V}}_i^J + \eta\mathbf{V}_i - \frac{T_i}{S_i}\sum_{s\in\mathcal{S}_i}\mathbf{H}_{\tau_i^s}^H(\mathbf{H}_{\tau_i^s}\tilde{\mathbf{V}}_i^J - \mathbf{D}_{\tau_i^s})}{\alpha+\eta+[Q_{i+1}+\gamma T_i g(\mathbf{V}_i)]\gamma T_{i+1}}$.

The computational complexities of our online precoding solutions in (59) and (61) are dominated by matrix multiplications. They are in the order of $\mathcal{O}(NK^2)$.

Remark 10. Note that additional short-term per-antenna transmit power constraints can be incorporated in the convex set $\mathcal{V}_0$. In this case, both precoder optimization problems can be equivalently decomposed into N subproblems, each with a closed-form solution similar to (59) and (61).

C. Performance Bounds

We assume that the channel gain is bounded by a constant $B > 0$ at any time t, given by

$$\|\mathbf{H}_t\|_F \leq B, \quad \forall t \in \mathcal{T}. \tag{62}$$

We show in the following lemma that our online MIMO network virtualization problem satisfies the OCO Assumptions 1-4 made in Section IV-B. The proof follows from the above bound on $\mathbf{H}_t$ and the short-term transmit power limit on both $\mathbf{V}_t$ and $\mathbf{W}_t$, and is omitted for brevity.

Lemma 6. Assume the bounded channel gain in (62). Then, Assumptions 1-4 hold with the corresponding constants given by $\varrho = 2$, $L = B^2$, $D = 4B^2\sqrt{P_{\max}}$, $\beta = 2\sqrt{P_{\max}}$, $G = \sqrt{\max\{\bar{P}^2, (P_{\max} - \bar{P})^2\}}$, $\epsilon = \bar{P}$, and $R = 2\sqrt{P_{\max}}$.

From the results in Theorems 1-4, the performance bounds yielded by $\{\mathbf{V}_i\}$ are given by (25)-(44) and (48), with the corresponding $\varrho, L, D, \beta, G, \epsilon, R$ given in Lemma 6.

VI. Simulation Results

In this section, we present simulation results for applying PQGA to online precoding-based massive MIMO network virtualization, under typical urban micro-cell LTE network settings. We study the impact of various system parameters on algorithm convergence and performance. We numerically demonstrate the performance advantage of PQGA over the known best alternative.

A. Simulation Setup

We consider an urban hexagon micro-cell of radius 500 m. An InP owns the BS, which is equipped with $N = 32$ antennas as default. The InP performs network virtualization and serves $M = 4$ SPs. We focus on some arbitrary channel over one subcarrier with bandwidth $B_W = 15$ kHz. Within this channel, each SP $m \in \mathcal{M}$ serves $K_m = 2$ users uniformly distributed in the cell, for a total of $K = 8$ users in the cell. We set maximum transmit power limit $P_{\max} = 33$ dBm, time-averaged transmit power limit $\bar{P} = 30$ dBm, noise power spectral density $N_0 = -174$ dBm/Hz, and noise figure $N_F = 10$ dB, as default system parameters.

We model the fading channel as a first-order Gaussian-Markov process $\mathbf{h}_{t+1}^k = \alpha_{\mathbf{h}} \mathbf{h}_t^k + \mathbf{z}_t^k, \forall k \in \mathcal{K} = \{1, \ldots, K\}$, where $\mathbf{h}_t^k \sim \mathcal{CN}(\mathbf{0}, \beta_k \mathbf{I})$, with $\beta_k[\text{dB}] = -31.54 - 33 \log_{10}(d_k) - \psi_k$ capturing the path-loss and shadowing, d_k being the distance from the BS to user k, $\psi_k \sim \mathcal{CN}(0, \sigma_\phi^2)$ accounting for the shadowing effect with $\sigma_\phi = 8$ dB, $\alpha_{\mathbf{h}} \in [0, 1]$ is the channel correlation coefficient, and $\mathbf{z}_t^k \sim \mathcal{CN}(\mathbf{0}, (1 - \alpha_{\mathbf{h}}^2)\beta_k \mathbf{I})$ is independent of $\mathbf{h}_t^k$. We set $\alpha_{\mathbf{h}} = 0.997$ as default, which corresponds to pedestrian user speed 1 m/s, under the standard LTE transmission structure [40]. [5] We set the time slot duration $\Delta t = \frac{1}{B_W}$, such that an update period of 8 time slots is similar to one resource block time duration in LTE. We set the time horizon $T = 400$.

We assume that each SP $m \in \mathcal{M}$ uses zero forcing (ZF) precoding scheme $\varpi_t^m \mathbf{H}_t^{mH} (\mathbf{H}_t^m \mathbf{H}_t^{mH})^{-1}$ to design its virtual precoding matrix $\mathbf{W}_t^m$, where ϖ_t^m is a power normalizing factor such that $\|\mathbf{W}_t^m\|_F^2 = P_m = \frac{P_{\max}}{M}$. For performance evaluation, we define the time-averaged precoding deviation normalized against the virtualization demand as

$$\bar{f}(T) \triangleq \frac{1}{T} \sum_{i \in \mathcal{I}} \sum_{t \in \mathcal{T}_i} \frac{f_t(\mathbf{V}_i)}{\|\mathbf{D}_t\|_F^2},$$

[5] We emphasize here that the Gauss-Markov channel model is used for illustration only. PQGA can be applied to any arbitrary wireless environment, and the InP does not need to know the channel statistics.

the time-averaged transmit power as

$$\bar{P}(T) \triangleq \frac{1}{T}\sum_{i\in\mathcal{I}} T_i \|\mathbf{V}_i\|_F^2,$$

and the time-averaged per-user rate as

$$\bar{R}(T) \triangleq \frac{1}{TK}\sum_{i\in\mathcal{I}}\sum_{t\in\mathcal{T}_i}\sum_{k\in\mathcal{K}} \log_2\left(1+\text{SINR}_t^{ik}\right)$$

where $\text{SINR}_t^{ik} = \frac{|\mathbf{h}_t^{k\,T}\mathbf{v}_i^k|^2}{\sum_{j\neq k, j\in\mathcal{K}}|\mathbf{h}_t^{k\,T}\mathbf{v}_i^j|^2+\sigma_n^2}$, with $\mathbf{h}_t^k$ and $\mathbf{v}_i^k$ being the channel vector at time slot t and precoding vector in the i-th update period for user k, and $\sigma_n^2 = N_0 B_W + N_F$ being the noise power.

B. Impact of Update Periods

We first consider the update periods $\{T_i\}$ are fixed over time and there is only one CSI feedback at the beginning of each update period i. Fig. 3 shows $\bar{f}(T)$, $\bar{P}(T)$, and $\bar{R}(T)$ versus T with different values of the update period T_i. We observe that PQGA converges fast. The performance of PQGA deteriorates as T_i increases, *i.e.,* precoder updates are less frequent. This illustrates the impact of channel variation over time, while the precoder is fixed. The long-term transmit power $\bar{P}(T)$ quickly converges to the average transmit power limit $\bar{P}$.

C. Impact of Number of Aggregated Gradient Descent Steps

Fig. 4 shows $\bar{f}(T)$, $\bar{P}(T)$ and $\bar{R}(T)$ versus T for different numbers of the aggregated gradient descent steps J, with fixed update period $T_i = 8$ and one CSI feedback. The system performance improves as J increases, showing the performance gain brought by performing multi-step gradient descent. The impact of J on the long-term transmit power $\bar{P}(T)$ is small. We observe that the system performance almost stabilizes when $J = 8$. In the simulation results presented below, we set $J = 8$ as default parameter for PQGA.

D. Performance Comparison

For comparison, we consider the following method and performance benchmarks.

- *Yu et al.:* The InP runs the online algorithm from [22], which achieves the known best $\mathcal{O}(T^{\frac{1}{2}})$ static regret and $\mathcal{O}(1)$ constraint violation bounds. It has been demonstrated in [22] that this algorithm outperforms the ones in [18] and [19]. Note that [22] considers only

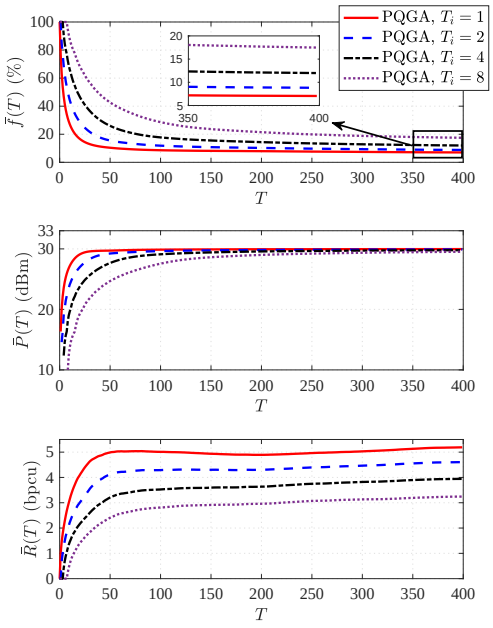


Fig. 3. $\bar{f}(T)$, $\bar{P}(T)$, and $\bar{R}(T)$ vs. T with different T_i values.

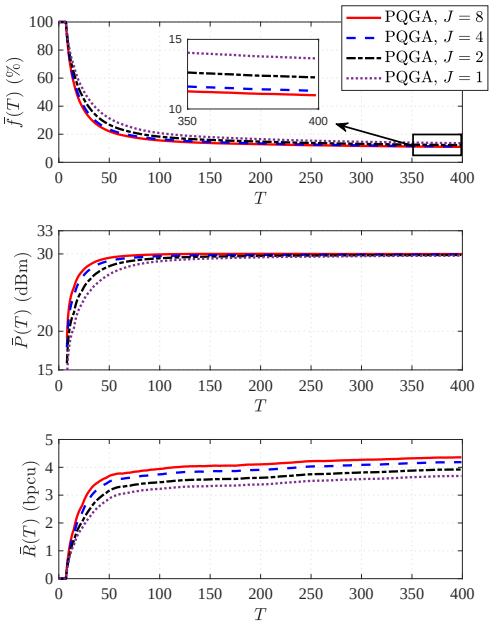


Fig. 4. $\bar{f}$(T), $\bar{P}(T)$, and $\bar{R}(T)$ vs. T with different J values.

the standard OCO setting with per-time-slot updates. In order to apply it to the periodic update scenario of our work, we treat each update period of T_i time slots as one super time slot. Furthermore, [22] considers only one gradient feedback at each time slot. Therefore, if there are multiple CSI feedbacks in an update period, we treat the averaged gradient as the gradient feedback.

- *Per-period optimal:* At the beginning of each update period i, the InP has the CSI feedbacks from the current update period i, and it implements $\mathbf{V}_i^{\circ}$ in (5).
- *Delayed optimal:* At the beginning of each update period i, the InP collects the delayed CSI feedbacks from the previous update period $i-1$, and it implements $\mathbf{V}_{i-1}^{\circ}$ in (5).
- *Offline fixed:* The InP has all the CSI feedbacks over I update periods in hindsight, and implements $\mathbf{V}^{\star}$ in (3) at each update period i.

We assume the update periods $\{T_i\}$ keep switching between 8 and 4 time slots. When $T_i = 8$, there are two CSI feedbacks at the first and fifth time slot, *i.e.,* $S_i = 2$. Otherwise, there is only one CSI feedback at the first time slot, *i.e.,* $T_i = 4$ and $S_i = 1$. Therefore, both the update periods $\{T_i\}$ and the numbers of CSI feedbacks $\{S_i\}$ are time varying.

In Fig. 5, we compare the steady-state precoding deviation $\bar{f}$ and per-user rate $\bar{R}$ between PQGA, Yu et al., per-period optimal, delayed optimal, and offline fixed, with different values of the channel correlation coefficient $\alpha_{\mathbf{h}}$. There is a large performance gap between the per-period optimal in (5) and the offline fixed in (3), indicating that the commonly used static benchmark

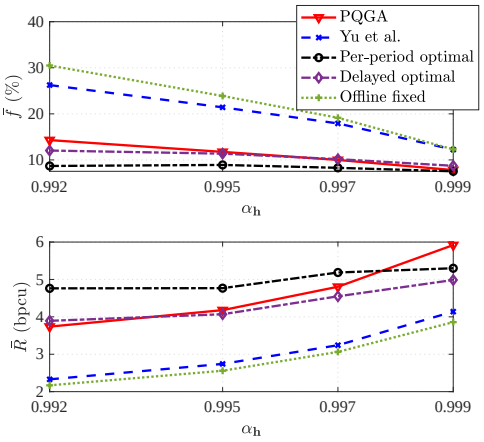


Fig. 5. Performance comparison on $\bar{f}$ and $\bar{R}$ vs. $\alpha_{\mathbf{h}}$.

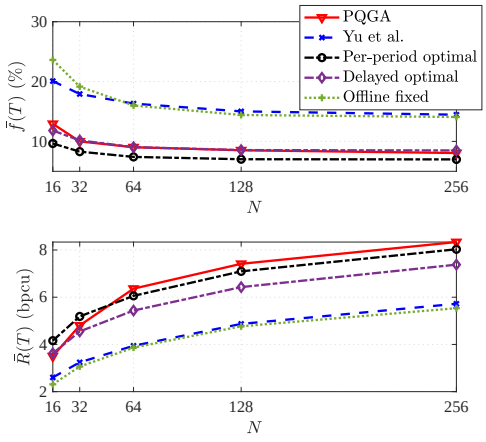


Fig. 6. Performance comparison on $\bar{f}$ and $\bar{R}$ vs. N.

for OCO may not be a meaningful comparison target in practical time-varying systems.

As $\alpha_{\mathbf{h}}$ increases, the performance of PQGA improves, since the channel states correlate more over time and the accumulated system variation decreases. When $\alpha_{\mathbf{h}} > 0.993$, which corresponds to pedestrian speed 2.5 m/s, $\bar{f}$ yielded by PQGA becomes smaller than the one produced by the delayed optimal. Note that the per-period optimal has the current CSI and can be shown to have a semi-closed-form solution. In contrast, PQGA only uses the delayed CSI and has a closed-form solution with lower computational complexity. As $\alpha_{\mathbf{h}}$ increases, $\bar{f}$ yielded by PQGA can approach to the one yielded by the per-period optimal. Furthermore, it is more robust to channel variation compared with the one yielded by Yu et al. under the periodic update setting. Note that the per-user rate $\bar{R}$ is not our precoding optimization objective, and thus is not directly related to $\bar{f}$. Furthermore, the per-period optimal needs to satisfy the long-term transmit power limit at each update period. As a side benefit, PQGA achieves a higher $\bar{R}$ than the per-period optimal when $\alpha_{\mathbf{h}}$ is large.

With the same setting, Fig. 6 shows the impact of the number of antennas N on the performance of PQGA and the benchmarks. As N increases, the InP has more freedom in choosing the antennas for downlink beamforming to mitigate the inter-SP interference, and thus the deviation from the virtualization demand $\bar{f}$ decreases. As N increases, $\bar{f}$ yielded by PQGA becomes smaller than the delayed optimal and approaches to the per-period optimal. Furthermore, the per-user rate $\bar{R}$ of PQGA is higher than the one yielded by the per-period optimal when N is large. PQGA substantially outperforms Yu et al. in a wide range of N values.

VII. Conclusions

This paper considers a new constrained OCO problem with periodic updates, where the gradient feedbacks may be partly missing over some time slots and the online decisions are updated over intervals that last for multiple time slots. We present an efficient algorithm termed PQGA, which uses periodic queues together with gradient aggregation to handle the possibly time-varying delay between decision epoches. Our analysis considers the impact of the constraint penalty structure and possibly multi-step aggregated gradient descent on the performance guarantees of PQGA, to provide bounds on its dynamic regret, static regret, and constraint violation. We apply PQGA to online network virtualization in massive MIMO systems. In addition to the benefits in terms of regret and constraint violation bounds, our simulation results further demonstrate the effectiveness of PQGA in terms of average system performance.

References

[1] J. Wang, B. Liang, M. Dong, and G. Boudreau, "Online MIMO wireless network virtualization over time-varying channels with periodic updates," in *Proc. IEEE Intel. Workshop on Signal Process. Advances in Wireless Commun. (SPAWC)*, 2020.

[2] N. Cesa-Bianchi and G. Lugosi, *Prediction, Learning, and Games*. Cambridge University Press, 2006.

[3] S. Shalev-Shwartz, "Online learning and online convex optimization," *Found. Trends Mach. Learn.*, vol. 4, pp. 107–194, Feb. 2012.

[4] P. Mertikopoulos and A. L. Moustakas, "Learning in an uncertain world: MIMO covariance matrix optimization with imperfect feedback," *IEEE Trans. Signal Process.*, vol. 64, pp. 5–18, Jan. 2016.

[5] M. Lin, A. Wierman, L. L. H. Andrew, and E. Thereska, "Dynamic right-sizing for power-proportional data centers," *IEEE/ACM Trans. Netw.*, vol. 21, pp. 1378–1391, Oct. 2013.

[6] Y. Zhang, M. H. Hajiesmaili, S. Cai, M. Chen, and Q. Zhu, "Peak-aware online economic dispatching for microgrids," *IEEE Trans. Smart Grid*, vol. 9, pp. 323–335, Jan. 2018.

[7] M. Zinkevich, "Online convex programming and generalized infinitesimal gradient ascent," in *Proc. Intel. Conf. Mach. Learn. (ICML)*, 2003.

[8] 3GPP TS38.300, "3rd Generation Partnership Project Technical Specification Group Radio Access Network; NR; NR and NG-RAN Overall Description; Statge 2 (Release 15)."

[9] B. Liang, "Mobile edge computing," in *Key Technologies for 5G Wireless Systems*. V. W. S. Wong, R. Schober, D. W. K. Ng, and L.-C. Wang, Eds., Cambridge University Press, 2017.

[10] E. Hazan, A. Agarwal, and S. Kale, "Logarithmic regret algorithms for online convex optimization," *Mach. Learn.*, vol. 69, pp. 169–192, 2007.

[11] J. Langford, A. J. Smola, and M. Zinkevich, "Slow learners are fast," in *Proc. Adv. Neural Info. Proc. Sys. (NIPS)*, 2009.

[12] K. Quanrud and D. Khashabi, "Online learning with adversarial delays," in *Proc. Adv. Neural Info. Proc. Sys. (NIPS)*, 2015.

[13] E. C. Hall and R. M. Willett, "Online convex optimization in dynamic environments," *IEEE J. Sel. Topics Signal Process.*, vol. 9, pp. 647–662, Jun. 2015.

[14] A. Jadbabaie, A. Rakhlin, S. Shahrampour, and K. Sridharan, "Online optimization : Competing with dynamic comparators," in *Proc. Intel. Conf. Artif. Intell. Statist. (AISTATS)*, 2015.

[15] A. Mokhtari, S. Shahrampour, A. Jababaie, and A. Ribeiro, "Online optimization in dynamic environments: Improved regret rates for strongly convex problems," in *Proc. IEEE Conf. Decision Control (CDC)*, 2016.

[16] L. Zhang, T. Yang, J. Yi, R. Jin, and Z. Zhou, "Improved dynamic regret for non-degenerate functions," in *Proc. Adv. Neural Info. Proc. Sys. (NIPS)*, 2017.

[17] R. Dixit, A. S. Bedi, R. Tripathi, and K. Rajawat, "Online learning with inexact proximal online gradient descent algorithms," *IEEE Trans. Signal Process.*, vol. 67, pp. 1338–1352, 2019.

[18] M. Mahdavi, R. Jin, and T. Yang, "Trading regret for efficiency: Online convex optimization with long term constraints," *J. Mach. Learn. Res.*, vol. 13, pp. 2503–2528, Sep. 2012.

[19] R. Jenatton, J. Huang, and C. Archambeau, "Adaptive algorithms for online convex optimization with long-term constraints," in *Proc. Intel. Conf. Mach. Learn. (ICML)*, 2016.

[20] X. Cao, J. Zhang, and H. V. Poor, "Impact of delays on constrained online convex optimization," in *Proc. Asilomar Conf. Signal Sys. Comput.*, 2019.

[21] T. Chen, Q. Ling, and G. B. Giannakis, "An online convex optimization approach to proactive network resource allocation," *IEEE Trans. Signal. Process.*, vol. 65, pp. 6350–6364, Dec. 2017.

[22] H. Yu and M. J. Neely, "A low complexity algorithm with $O(\sqrt{T})$ regret and $O(1)$ constraint violations for online convex optimization with long term constraints," *J. Mach. Learn. Res.*, vol. 21, pp. 1–24, Feb. 2020.

[23] H. Yu, M. J. Neely, and X. Wei, "Online convex optimization with stochastic constraints," in *Proc. Adv. Neural Info. Proc. Sys. (NIPS)*, 2017.

[24] X. Cao, J. Zhang, and H. V. Poor, "A virtual-queue-based algorithm for constrained online convex optimization with applications to data center resource allocation," *IEEE J. Sel. Topics Signal Process.*, vol. 12, pp. 703–716, Aug. 2018.

[25] J. Wang, B. Liang, M. Dong, G. Boudreau, and H. Abou-Zeid, "Delay-tolerant constrained OCO with application to network resource allocation," in *Proc. IEEE Conf. Comput. Commun. (INFOCOM)*, 2021.

[26] M. J. Neely, *Stochastic Network Optimization with Application on Communication and Queueing Systems*. Morgan & Claypool, 2010.

[27] M. J. Neely, "Dynamic optimization and learning for renewal systems," *IEEE Trans. Automat. Contr.*, vol. 58, pp. 32–46, 2013.

[28] M. Lotfinezhad, B. Liang, and E. S. Sousa, "Optimal control of constrained cognitive radio networks with dynamic population size," in *Proc. IEEE Conf. Comput. Commun. (INFOCOM)*, 2010.

[29] H. Yu and M. J. Neely, "Dynamic transmit covariance design in MIMO fading systems with unknown channel distributions and inaccurate channel state information," *IEEE Trans. Wireless Commun.*, vol. 16, pp. 3996–4008, Jun. 2017.

[30] J. Wang, M. Dong, B. Liang, and G. Boudreau, "Online precoding design for downlink MIMO wireless network virtualization with imperfect CSI," in *Proc. IEEE Conf. Comput. Commun. (INFOCOM)*, 2020.

[31] O. Besbes, Y. Gur, and A. Zeevi, "Non-stationary stochastic optimization," *Oper. Res.*, vol. 63, pp. 1227–1244, Sep. 2015.

[32] V. Jumba, S. Parsaeefard, M. Derakhshani, and T. Le-Ngoc, "Resource provisioning in wireless virtualized networks via massive-MIMO," *IEEE Wireless Commun. Lett.*, vol. 4, pp. 237–240, Jun. 2015.

[33] Z. Chang, Z. Han, and T. Ristaniemi, "Energy efficient optimization for wireless virtualized small cell networks with large-scale multiple antenna," *IEEE Trans. Commun.*, vol. 65, pp. 1696–1707, Apr. 2017.

[34] S. Parsaeefard, R. Dawadi, M. Derakhshani, T. Le-Ngoc, and M. Baghani, "Dynamic resource allocation for virtualized wireless networks in massive-MIMO-aided and fronthaul-limited C-RAN," *IEEE Trans. Veh. Technol.*, vol. 66, pp. 9512–9520, Oct. 2017.

[35] D. Tweed and T. Le-Ngoc, "Dynamic resource allocation for uplink MIMO NOMA VWN with imperfect SIC," in *Proc. IEEE Int. Conf. Commun. (ICC)*, 2018.

[36] Y. Liu, M. Derakhshani, S. Parsaeefard, S. Lambotharan, and K. Wong, "Antenna allocation and pricing in virtualized massive MIMO networks via Stackelberg game," *IEEE Trans. Commun.*, vol. 66, pp. 5220–5234, Nov. 2018.

[37] K. Zhu and E. Hossain, "Virtualization of 5G cellular networks as a hierarchical combinatorial auction," *IEEE Trans. Mobile Comput.*, vol. 15, pp. 2640–2654, Oct. 2016.

[38] J. Wang, M. Dong, B. Liang, and G. Boudreau, "Online downlink MIMO wireless network virtualization in fading environments," in *Proc. IEEE Global Telecommun. Conf. (GLOBECOM)*, 2019.

[39] S. Boyd and L. Vandenberghe, *Convex Optimization*. Cambridge University Press, 2004.

[40] H. Holma and A. Toskala, *WCDMA for UMTS - HSPA evolution and LTE*. John Wiely & Sons, 2010.